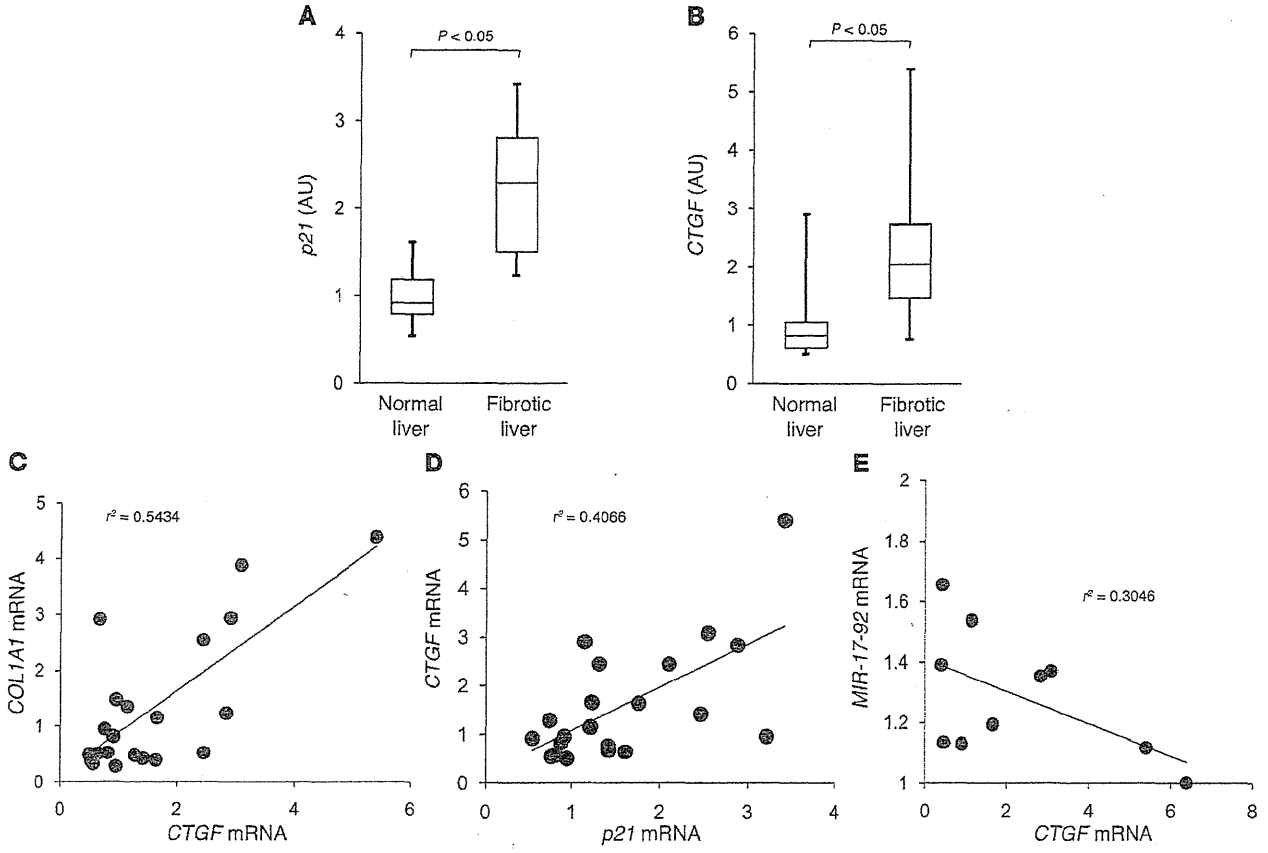

Figure 9

p53-regulated gene expression increases in fibrotic human liver and is correlated with an increase in *CTGF* gene expression. (**A** and **B**) A total of 21 non-tumorous human liver samples were subdivided into two groups histologically defined as normal liver and fibrotic liver. *p21* (**A**) and *CTGF* (**B**) mRNA levels in the liver were determined by real-time RT-PCR; $n = 11$ (normal liver group) and $n = 10$ (fibrotic liver group). (**C** and **D**) *COL1A1*, *CTGF*, and *p21* mRNA levels in the liver of 21 non-tumorous human liver samples were determined by real-time RT-PCR and plotted to analyze the correlation between *COL1A1* and *CTGF* ($P < 0.01$) (**C**) or between *CTGF* and *p21* ($P < 0.01$) (**D**). (**E**) *miR-17-92* and *CTGF* mRNA levels in the liver of 10 human fibrotic liver samples were determined by real-time RT-PCR and plotted to analyze the correlation between them ($P < 0.01$).

change upon nutlin-3a treatment in HepG2 cells (Figure 8A), suggesting that the post-transcriptional regulation may be involved in the p53-induced CTGF upregulation. Recently, epigenetic regulation of the *CTGF* gene has been demonstrated (30-32), and the *miR-17-92* cluster gene, in particular, has been reported to repress CTGF synthesis in murine colonocytes and human glioblastoma cells (31, 32). Upon nutlin-3a treatment, expression of the *miR-17-92* cluster gene decreased in HepG2 cells (Figure 8B), indicating that p53 activation reduced *MIR-17-92* gene expression in HepG2 cells. The miR-17-92 cluster comprises 7 miRNAs that are transcribed as a single polycistronic unit (31, 33), and in silico analysis revealed that, among these miRNAs, *MIR18A*, *MIR19A*, and *MIR19B* can be predicted to target CTGF. Real-time RT-PCR study revealed that the gene expression of these 3 miRNAs also decreased upon nutlin-3a treatment in HepG2 cells (Figure 8C). Introduction of the antisense of these 3 miRNAs increased CTGF synthesis in HepG2 cells (Figure 8D), indicating that they suppressed CTGF synthesis in HepG2 cells. To investigate the causal involvement of down-regulation of the miRNAs in p53-induced CTGF upregulation, we administered precursors of the miRNAs to HepG2 cells, and CTGF synthesis was examined upon nutlin-3a treatment. In contrast to negative control miRNA, administration of these miRNAs inhibited the upregulation of CTGF upon nutlin-3a treatment (Figure 8E), suggesting that a decrease in miR-18a, miR-19a, and miR-19b in the *miR-17-92* cluster was involved in the mechanism of CTGF upregulation by p53. To investigate the involvement of the miR-17-92 cluster in CTGF upregulation in hepatocytes of Mdm2-knockout mice, we examined hepatocyte gene expression of the *miR-17-92* cluster and found it to be significantly lower in the knockout mice than in the control littermates (Figure 8F), suggesting that the miR-17-92 cluster may be involved in p53-mediated CTGF upregulation in hepatocytes of the knockout mice.

p53-regulated gene expression increases in the human fibrotic liver and is correlated with an increase in Ctgf gene expression. Finally, to investigate the relationship between p53 activation and human liver fibrosis, we examined the expression of p53-regulated genes and fibrosis-related genes in human liver samples. *p21* gene expression increased in the fibrotic liver and was significantly higher than in the normal liver (Figure 9A). We observed that *NOXA* gene expression in the fibrotic liver was also significantly higher than in the normal liver (Supplemental Figure 10). These findings suggested that p53 may be transcriptionally active in the fibrotic

liver. Regarding fibrosis-related genes, *CTGF* gene expression was significantly higher in the fibrotic liver than in the normal liver (Figure 9B). The increase in *CTGF* gene expression paralleled the increase in *COL1A1* gene expression, with a significant correlation between them (Figure 9C). These results suggested that CTGF may be involved in the progression of human liver fibrosis. There was a significant correlation between the gene expression of *p21* and *CTGF* (Figure 9D), suggesting that p53 activation might be involved in the upregulation of CTGF and the progression of liver fibrosis in humans. We also found that there was a significant negative correlation between the gene expression of *CTGF* and the *miR-17-92* cluster in the fibrotic liver (Figure 9E), suggesting the involvement of the miR-17-92 cluster in the p53/CTGF pathway in the human fibrotic liver.

Discussion

In the present study, to investigate the role of p53 in liver fibrosis, we generated hepatocyte-specific Mdm2-knockout mice and found a direct link between p53 activation in parenchymal cells and organ fibrosis. In unstressed cells, expression of p53 is tightly regulated and maintained at a low level by binding with a variety of proteins that promote p53 degradation via the ubiquitin/proteasome pathway (13). Among these p53 inhibitory proteins, Mdm2 is critically important for this process, since Mdm2-knockout mice show embryonic lethality but were fully rescued by deletion of *p53* (34). When Cre-mediated conditional Mdm2-knockout mice were generated and studied, the findings revealed that *Mdm2* deletion only in the central nervous system or the heart still led to embryonic lethality due to massive apoptosis, and this could also be rescued by deletion of *p53* (15, 35). These findings demonstrated that Mdm2 functions as a crucial and specific p53 inhibitor in a variety of organs. In the present study, using hepatocyte-specific Mdm2-knockout mice, we could observe the consequences of persistent p53 activation in hepatocytes and discover the profibrotic function of p53.

Regarding the mechanism(s) involving spontaneous liver fibrosis in our Mdm2-knockout mice, we observed a mild increase in hepatocyte apoptosis (Figure 3, A–E). We have previously reported that hepatocyte-specific knockout of either Bcl-xL or Mcl-1, major anti-apoptotic Bcl-2 family proteins, causes massive hepatocyte apoptosis and leads to liver fibrosis in mice (16, 36). Thus, although apoptosis is generally considered to be quiescent cell death that does not cause organ injury, hepatocyte apoptosis is apparently involved in liver fibrogenesis. However, in these mice, liver fibrosis is not evident at 6 weeks of age, although they show much higher ALT levels, more than 300 IU/ml, and seem to have much more apoptosis than hepatocyte-specific Mdm2-knockout mice. Moreover, when hepatocyte apoptosis was similarly induced in Mdm2-knockout mice and control littermates by administration of ABT-737, a Bcl-xL inhibitor that causes mild hepatocyte apoptosis in vivo (refs. 21, 22, and Supplemental Figure 11A), additional liver fibrogenic responses occurred in the knockout mice but not in the control littermates (Supplemental Figure 11B). Based on these findings, hepatocyte apoptosis could contribute to liver fibrosis, but some additional factors should be required for the liver fibrosis observed in the Mdm2-knockout mice.

In Mdm2-knockout mice, we also found an upregulation of CTGF synthesis in hepatocytes (Figure 7, A and B). CTGF, also known as CCN family 2 (CCN2), is one of the CCN family proteins and plays a pivotal role in fibrosis in the lung, skin, kidney, and heart (37) through extracellular matrix production, cell cycle control, and cell adhesion and migration (14, 38, 39). With respect to the liver, several publications have reported that CTGF expression increases in human chronic liver fibrotic diseases such as chronic hepatitis C, NASH, and liver cirrhosis (40–43). Moreover, previous studies have shown that CTGF inhibition by siRNA had a beneficial effect on experimental liver fibrosis (44, 45), indicating that CTGF functions as an important profibrogenic cytokine in the liver. Although the main source of CTGF was thought to be HSCs and fibroblasts (46), recent reports have revealed that CTGF is also produced from hepatocytes (47, 48). Furthermore, transgenic mice expressing CTGF under the control of the albumin gene promoter showed exacerbation of liver fibrosis induced by chronic CCl_4 administration (49), demonstrating that hepatocyte-derived CTGF plays an important role in liver fibrogenesis. However, Tong et al. (49) have also reported that hepatocyte-specific CTGF transgenic mice did not show spontaneous fibrosis in the liver without any fibrotic stimuli. Taken together, these findings support the idea that CTGF produced from hepatocytes may be an important factor for promoting liver fibrosis in the presence of apoptotic stimuli in Mdm2-knockout mice.

To further examine this idea, we performed an in vitro study using murine HSCs cocultured with apoptotic bodies prepared from hepatocytes. In agreement with a previous report (50), hepatocyte-derived apoptotic bodies efficiently activated HSCs (Supplemental Figure 12), and CTGF administration significantly upregulated type I collagen synthesis in HSCs in combination with apoptotic bodies (Supplemental Figure 13). Based on these results and in vivo findings, we suggest that hepatocyte p53 activation increased hepatocyte apoptosis and CTGF synthesis, and both together may induce HSC activation and collagen synthesis, contributing to the development of spontaneous liver fibrosis in Mdm2-knockout mice. It should be noted here that p53 activation did not appear to be a single causal factor for inducing apoptosis in two independent models of murine liver fibrosis but was a required for CTGF expression. Since CTGF expression was well correlated with p53 activation and liver fibrosis in human livers, p53-mediated CTGF induction may be a novel and important pathway for promoting liver fibrosis.

The Alb-Cre transgenic mice expressed cre recombinase in intrahepatic cholangiocytes as well as hepatocytes, as observed from β-galactosidase staining of the liver sections in Alb-Cre and Rosa26-LacZ double-transgenic mice (data not shown). In the present study, Mdm2-knockout mice (*Mdm2$^{f/f}$alb-cre*) actually showed p53 accumulation and CTGF expression in some cholangiocytes (Supplemental Figure 14 and Figure 7B), and nutlin-3a treatment upregulated *CTGF* gene expression as well as p53-regulated genes in SNU-1079 cells, a human cholangiocellular carcinoma cell line with wild-type p53 status (ref. 51 and Supplemental Figure 15), suggesting the existence of the p53/CTGF pathway in cholangiocytes as well. However, CTGF expression was observed even in the cholangiocytes of control littermates, and its levels were not much different from those of the knockout mice (Figure 7B). Therefore, although cholangiocytes may contribute to hepatic CTGF synthesis in physiological settings, they may contribute less to the hepatic CTGF increase observed in Mdm2-knockout mice.

Recent research has shown that the *CTGF* gene is repressed by several miRNAs such as miR-18a, miR-30, and miR-133 (31, 32, 52, 53). In addition, a previous report has revealed that p53 represses *miR-17-92* transcription by binding to the p53-binding

site overlapping the TATA box in the *miR-17-92* promoter lesion (54). Thus, we focused on the miR-17-92 cluster (which includes miR-18) and identified a what we believe to be a novel regulatory mechanism by which p53 upregulates CTGF through repression of the *miR-17-92* cluster gene in hepatocytes, revealing the involvement of this mechanism not only in vitro, but also in rodents and fibrotic human liver.

In the present study, we demonstrated a direct causal link between p53 activation in hepatocytes and liver fibrosis, as evidenced by the spontaneous liver fibrosis of hepatocyte-specific Mdm2-knockout mice and the alleviation of diet- or TAA-induced liver fibrosis in hepatocyte-specific p53-knockout mice. In hepatocytes, p53 activation induced the expression of CTGF, a key regulator of liver fibrosis, through miRNA regulation. Analysis of human tissues provided evidence that the p53/CTGF axis may be involved in human liver fibrosis. Recently, therapeutic applications of a p53 inhibitor have been proposed for preventing radiation-induced adverse events that are mediated by p53 activation (55). CTGF was also reported to increase in a variety of tissues, such as the liver, intestine, and colon, upon irradiation (56, 57) and play an important role in the progression of radiation-induced fibrosis (57, 58). Our present study suggests the possibility that positive regulation of CTGF by p53 may be a therapeutic target of organ fibrosis caused by irradiation therapy as well as disease.

Methods

Cell lines and materials. Human hepatoma cell line HepG2 and murine normal hepatocyte cell line BNL CL.2 were obtained from ATCC, and human cholangiocellular carcinoma cell line SNU-1079 was obtained from the Korean Cell Line Bank (51). They were cultured at 37°C under 5% CO_2 in DMEM containing 10% FCS (Sigma-Aldrich). Nutlin-3a and Adriamycin were purchased from Sigma-Aldrich.

Human samples. Non-tumorous liver samples were obtained from 21 patients at surgical operation for hepatocellular carcinoma (HCC) (n = 10) and colorectal liver metastasis (n = 11). Among the 10 patients with HCC, 7 were positive for HCV antibody. Of the 10 patients, 4 were histologically diagnosed as having liver cirrhosis and 6 as having chronic hepatitis. The 11 metastatic patients were seronegative for both HBsAg and HCV antibodies. They all had normal liver function and were histologically diagnosed as non-fibrotic livers. The resected non-tumorous liver specimens were taken as far from the tumor as possible, soaked in RNAlater solution (Ambion), and then stored at –80°C until use. Written informed consent was obtained from all patients according to a protocol approved by the Institutional Research Board of Osaka University Hospital.

Mice. *Mdm2*$^{f/f}$ mice were provided by Guillermina Lozano (University of Texas MD Anderson Cancer Center, Houston, Texas, USA) (15). Hepatocyte-specific Mdm2-knockout mice (*Mdm2*$^{f/f}$*alb-cre*) were generated by mating of *Mdm2*$^{f/f}$ mice and Alb-Cre transgenic mice (16, 21). *Trp53*$^{f/f}$ mice and ROSA26-LacZ mice were purchased from The Jackson Laboratory. Hepatocyte-specific Trp53-knockout mice (*Trp53*$^{f/f}$*alb-cre*) were generated by mating *Trp53*$^{f/f}$ mice and *alb-cre* transgenic mice. Hepatocyte-specific Mdm2- and Trp53-double-knockout mice (*Mdm2*$^{f/f}$*Trp53*$^{f/f}$*alb-cre*) were generated by mating *Mdm2*$^{f/f}$*Trp53*$^{f/+}$ mice and *Mdm2*$^{f/f}$*Trp53*$^{f/+}$*alb-cre* mice. Genomic recombination of the *Mdm2* and *Trp53* genes occurred at a rate of about 75% in the entire liver (data not shown). C57BL/6J mice and BALB/c mice were purchased from Charles River Laboratories Japan. They were maintained in a specific pathogen-free facility and treated with humane care with approval from the Animal Care and Use Committee of Osaka University Medical School.

Isolation and culture of murine hepatocytes and NPCs. Hepatocytes and NPCs were isolated from *Mdm2*$^{f/f}$ mice and *Mdm2*$^{f/f}$*alb-cre* mice by 2-step collagenase-pronase perfusion of mouse livers as previously described (17). Isolated hepatocytes were maintained at 37°C under 5% CO_2 in William's Eagle medium containing 10% FCS (Sigma-Aldrich), 100 nM dexamethasone, 100 nM insulin (Sigma-Aldrich) and L-glutamine (Invitrogen).

Histological analyses. The liver sections were stained with H&E. For detection of apoptotic cells, the liver sections were also subjected to TUNEL staining, according to a previously reported procedure (36). To assess their regenerative status, we stained liver sections for nuclear BrdU incorporation as previously described (59). To assess fibrosis, we stained the liver sections with picrosirius red. The percentage of collagen deposition was quantified using image analysis software (WinROOF visual system, Mitani Corp.) (59). For immunohistochemical detection of p53, α-SMA, cleaved caspase-3, and CTGF, the liver sections were respectively incubated with polyclonal rabbit anti-p53 antibody (Vector Laboratories Inc.), polyclonal rabbit anti-α-SMA antibody (Santa Cruz Biotechnology Inc.), polyclonal rabbit anti-cleaved caspase-3 antibody (Cell Signaling Technology Inc.), and polyclonal goat anti-CTGF antibody (Santa Cruz Biotechnology Inc.).

Senescence-associated β-galactosidase assay. To assess hepatocyte senescence, we performed a senescence-associated β-galactosidase assay according to a previously described procedure (60). Briefly, the frozen liver sections were fixed in 0.25% glutaraldehyde for 10 minutes and immersed overnight in SA-β-gal staining solution (0.5 mg/ml X-gal, 3 mM potassium ferricyanide, 3 mM potassium ferrocyanide, 2 mM $MgCl_2$, 0.25% Triton X-100, 0.1 M phosphate buffer, pH 6.0).

Determination of liver hydroxyproline content. Hydroxyproline content was determined essentially as described previously (59). Results are expressed as micrograms of hydroxyproline per gram of wet liver.

Western blot analysis. Liver tissue was lysed in lysis buffer (1% Nonidet P-40, 0.5% sodium deoxycholate, 0.1% sodium dodecyl sulfate, 1× protease inhibitor cocktail [Nacalai tesque], 1× phosphatase inhibitor cocktail [Nacalai tesque], phosphate-buffered saline, pH 7.4). The liver lysates were cleared by centrifugation at 10,000 *g* at 4°C for 15 minutes. The protein concentrations were determined using a bicinchoninic acid protein assay kit (Pierce). Equal amounts of protein lysates were electrophoretically separated by SDS polyacrylamide gels and transferred onto a polyvinylidene fluoride membrane. For immunodetection, the following antibodies were used: rabbit monoclonal antibody to p53, rabbit polyclonal antibody to Bax (Cell Signaling Technology), rabbit polyclonal antibody to p21, goat polyclonal antibody to CTGF, rabbit polyclonal antibody to p53 (Santa Cruz Biotechnology Inc.), rabbit polyclonal antibody to Noxa and p21 (Abcam), rabbit polyclonal antibody to Puma (ProSci Inc.), and mouse monoclonal antibody to β-actin (Sigma-Aldrich).

Real-time RT-PC for mRNA. Total RNA extracted from cell lines and liver tissues using the RNeasy Mini Kit (QIAGEN) was reverse transcribed and subjected to real-time RT-PCR as previously described (59). mRNA expression of the specific genes was quantified using TaqMan Gene Expression Assays (Applied Biosystems) as follows: murine Col1a1 (assay ID: Mm00801666_g1), murine Col1a2 (Mm01165187_m1), murine Ctgf (Mm01192933_g1), murine Pmaip1 (Mm00451763_m1), murine Cdkn1a (Mm01303209_m1), murine Bax (Mm0043205_m1), murine Trp53 (Mm01731287_m1), murine Tgfb1 (Mm01178820_m1), murine Pdgfb (Mm01298578_m1), murine Mmp2 (Mm00439506_m1), murine Mmp14 (Mm01318969_g1), murine Timp1 (Mm01341361_m1), murine Acta2 (Mm01546133_m1), murine miR-17-92 (Mm03307063_pri), murine Actb (Mm02619580_g1), human COL1A1 (Hs01076777_m1), human CTGF (Hs00170014_m1), human PMAIP1 (Hs00560402_m1), human CDKN1A (Hs00355782_m1), human TP53 (Hs01034249_m1), human TGFB1 (Hs00998133_m1), human PDGFB (Hs00234042_m1), human BBC3 (Hs00248075_m1), human

BAX (Hs00180269_m1), and human ACTB (Hs99999903_m1). Human pri-miR-17-92 expression was quantified using the primers described previously (54). Transcript levels are presented as fold change.

Caspase-3/7 activity. Serum caspase-3/7 activity was measured with a luminescence substrate assay for caspase-3 and caspase-7 (Caspase-Glo assay, Promega) as described previously (61).

Real-time RT-PCR assays for mature miRNA. Total RNA including the miRNA fraction extracted from cell lines using the miRNeasy Mini Kit (QIAGEN) was reverse transcribed. Quantitative PCR was performed with TaqMan MicroRNA Assays (Applied Biosystems) specific for *miR-18a* (assay ID: 002422), *miR-19a* (assay ID: 000395), and *miR-19b* (assay ID: 000396). To normalize the expression levels of miRNAs, we used the TaqMan MicroRNA Assay specific for RNU6B (assay ID: 001093) as the endogenous control. Transcript levels are presented as fold change.

Transfections with miRNA. HepG2 cells were transfected with 10 nM Pre-miR miRNA precursor molecules (Ambion) of *MIR18A* (PM12973), *MIR19A* (PM10649), and *MIR19B* (PM10629) using RNAiMAX (Invitrogen) according to the manufacturer's instructions. Pre-miR negative control (Ambion) was used as a control.

Transfections with antisense of miRNA. HepG2 cells were transfected with 100 nM Anti-miR miRNA inhibitor (Ambion) of *MIR18A* (AM12973), *MIR19A* (AM10649) and *MIR19B* (AM10629) using RNAiMAX (Invitrogen) according to the manufacturer's instructions. Anti-miR negative control (Ambion) was used as a control.

Dual luciferase reporter assay. Plasmid pTS-589, which contains the *CTGF* promoter linked to the upstream of a firefly luciferase reporter gene (29), was transfected into HepG2 cells together with pRL-TK (Promega) using Lipofectamine LTX (Invitrogen). Upon 24 hours of Nutlin-3a (20 μM) or recombinant TGF-β (10 ng/ml) treatment, firefly luciferase activity was measured using the Luciferase Assay System (Promega) and normalized to *Renilla* luciferase activity.

siRNA-mediated knockdown. HepG2 cells were transfected with siRNA against *TP53* (Validated Stealth RNAi siRNA, oligo ID: VHS40367) (Invitrogen) using Lipofectamine RNAi-MAX (Invitrogen) according to the manufacturer's protocol. Stealth RNAi Negative Control Low GC (Invitrogen) was used as the control.

Isolation and culture of mouse HSCs. HSCs were isolated from C57BL/6J mice by 2-step collagenase-pronase perfusion of mouse liver, followed by density gradient centrifugation with 8.2% Nycodenz (Sigma-Aldrich) as previously described (59). Isolated HSCs were maintained at 37°C under 5% CO_2 in DMEM containing 10% FCS (Sigma-Aldrich). HSCs after a few passages were used for the experiments.

Generation of apoptotic body and coculture experiment with HSCs. Apoptotic bodies of hepatocytes were generated as described previously (50). Briefly, BNL CL.2 cells were UV irradiated (100 mJ/cm^2) and incubated for 2 days in DMEM with 10% FCS. Next, floating apoptotic bodies were collected and centrifuged at 1,500 *g* for 5 minutes. HSCs (1.0×10^5) were starved for 48 hours in DMEM without FCS and then cocultured with apoptotic bodies (4.0×10^5) in DMEM with 10% FCS for the indicated time courses with or without 100 ng/ml recombinant CTGF (EMP Genetech).

Experimental protocol for ABT-737 administration. ABT-737, provided by Abbott Laboratories, was dissolved with a mixture of 30% propylene glycol, 5% Tween 80, and 65% D5W (5% dextrose in water), to a final pH of 4–5 as described previously (21). ABT-737 (100 mg/kg) was intraperitoneally administered to C57BL/6J mice, and 2 days later they were sacrificed for the various analyses.

Experimental protocol for ATH diet feeding. C57BL/6J mice, *Trp53*$^{fl/fl}$ mice, and *Trp53*$^{fl/fl}$*alb-cre* mice were subdivided into two groups: (a) mice fed an ATH diet (1.25% [w/w] cholesterol, 0.5% [w/w] cholic acid, and 16% [w/w] fat) for 4 weeks and (b) mice given standard chow (CRF-1, Charles River Laboratories Japan) for 4 weeks. After having been fasted for 8 hours, the animals were sacrificed for the various analyses.

Experimental protocol for TAA intraperitoneal administration. TAA (200 mg/kg) (Sigma-Aldrich) was intraperitoneally administered to *Trp53*$^{fl/fl}$ mice and *Trp53*$^{fl/fl}$*alb-cre* mice 3 times per week for 6 weeks, and then the animals were sacrificed for the various analyses.

Experimental protocol for hydrodynamic injection of p53 expression plasmid. BALB/c mice were given injection of pORF9-mp53 plasmid, an expression vector containing the murine p53 open reading frame (Invivogen) or its control plasmid via the tail vein by a hydrodynamic injection procedure (28) and sacrificed 2 days later for the various analyses.

Statistics. Data are expressed as median and interquartile range or mean ± SD. Statistical analyses were performed by the unpaired Mann-Whitney *U* test or 1-way ANOVA unless otherwise indicated. When ANOVA analyses were applied, differences in the mean values among the groups were examined by Scheffe post hoc correction. Correlations were assessed using the Pearson product-moment correlation coefficient. *P* values less than 0.05 were considered statistically significant.

Acknowledgments

We thank Guillermina Lozano (University of Texas MD Anderson Cancer Center) for providing the floxed *Mdm2* mice. We also thank Abbott Laboratories for providing ABT-737. We thank Kanako Mori for help with experiments.

Received for publication August 31, 2010, and accepted in revised form May 12, 2011.

Address correspondence to: Tetsuo Takehara, Department of Gastroenterology and Hepatology, Osaka University Graduate School of Medicine, 2-2 Yamada-oka, Suita, Osaka 565-0871, Japan. Phone: 81.6.6879.3621; Fax: 81.6.6879.3629; E-mail: takehara@gh.med.osaka-u.ac.jp.

1. Vousden KH, Lu X. Live or let die: the cell's response to p53. *Nat Rev Cancer.* 2002;2(8):594–604.
2. Bensaad K, et al. TIGAR, a p53-inducible regulator of glycolysis and apoptosis. *Cell.* 2006;126(1):107–120.
3. Hu W, Zhang C, Wu R, Sun Y, Levine A, Feng Z. Glutaminase 2, a novel p53 target gene regulating energy metabolism and antioxidant function. *Proc Natl Acad Sci U S A.* 2010;107(16):7455–7460.
4. Crighton D, et al. DRAM, a p53-induced modulator of autophagy, is critical for apoptosis. *Cell.* 2006;126(1):121–134.
5. Tyner SD, et al. p53 mutant mice that display early ageing-associated phenotypes. *Nature.* 2002; 415(6867):45–53.
6. Minamino T, et al. A crucial role for adipose tissue p53 in the regulation of insulin resistance. *Nat Med.* 2009; 15(9):1082–1087.
7. Sano M, et al. p53-induced inhibition of Hif-1 causes cardiac dysfunction during pressure overload. *Nature.* 2007;446(7134):444–448.
8. Akyol G, et al. P53 and proliferating cell nuclear antigen (PCNA) expression in non-tumoral liver diseases. *Pathol Int.* 1999;49(3):214–221.
9. Panasiuk A, Dzieciol J, Panasiuk B, Prokopowicz D. Expression of p53, Bax and Bcl-2 proteins in hepatocytes in non-alcoholic fatty liver disease. *World J Gastroenterol.* 2006;12(38):6198–6202.
10. Attallah AM, Shiha GE, Ismail H, Mansy SE, El-Sherbiny R, El-Dosoky I. Expression of p53 protein in liver and sera of patients with liver fibrosis, liver cirrhosis or hepatocellular carcinoma associated with chronic HCV infection. *Clin Biochem.* 2009;42(6):455–461.
11. Loguercio C, et al. Liver p53 expression in patients with HCV-related chronic hepatitis. *J Viral Hepat.* 2003;10(4):266–270.
12. Papakyriakou P, et al. Apoptosis and apoptosis related proteins in chronic viral liver disease. *Apoptosis.* 2002;7(2):133–141.
13. Kruse JP, Gu W. Modes of p53 regulation. *Cell.* 2009;137(4):609–622.
14. Gressner OA, Gressner AM. Connective tissue growth factor: a fibrogenic master switch in fibrotic liver diseases. *Liver Int.* 2008;28(8):1065–1079.
15. Grier JD, Xiong S, Elizondo-Fraire AC, Parant JM, Lozano G. Tissue-specific differences of p53 inhibition by Mdm2 and Mdm4. *Mol Cell Biol.* 2006;26(1):192–198.
16. Takehara T, et al. Hepatocyte-specific disruption of Bcl-xL leads to continuous hepatocyte apoptosis and liver fibrotic responses. *Gastroenterology.*

2004;127(4):1189–1197.
17. Sakamori R, et al. Signal transducer and activator of transcription 3 signaling within hepatocytes attenuates systemic inflammatory response and lethality in septic mice. *Hepatology*. 2007;46(5):1564–1573.
18. Vassilev LT, et al. In vivo activation of the p53 pathway by small-molecule antagonists of MDM2. *Science*. 2004;303(5659):844–848.
19. Bataller R, Brenner DA. Liver fibrosis. *J Clin Invest*. 2005;115(2):209–218.
20. Friedman SL. Mechanisms of hepatic fibrogenesis. *Gastroenterology*. 2008;134(6):1655–1669.
21. Hikita H, et al. BH3-only protein bid participates in the Bcl-2 network in healthy liver cells. *Hepatology*. 2009;50(6):1972–1980.
22. Hikita H, et al. The Bcl-xL inhibitor, ABT-737, efficiently induces apoptosis and suppresses growth of hepatoma cells in combination with sorafenib. *Hepatology*. 2010;52(4):1310–1321.
23. Mitchell C, Willenbring H. A reproducible and well-tolerated method for 2/3 partial hepatectomy in mice. *Nat Protoc*. 2008;3(7):1167–1170.
24. Larter CZ, Yeh MM. Animal models of NASH: getting both pathology and metabolic context right. *J Gastroenterol Hepatol*. 2008;23(11):1635–1648.
25. Matsuzawa N, et al. Lipid-induced oxidative stress causes steatohepatitis in mice fed an atherogenic diet. *Hepatology*. 2007;46(5):1392–1403.
26. Safadi R, et al. Immune stimulation of hepatic fibrogenesis by CD8 cells and attenuation by transgenic interleukin-10 from hepatocytes. *Gastroenterology*. 2004;127(3):870–882.
27. Lin Y, et al. Tumour suppressor p53 and Rb genes in human hepatocellular carcinoma. *Ann Acad Med Singapore*. 1996;25(1):22–30.
28. Suzuki T, et al. Intravenous injection of naked plasmid DNA encoding hepatitis B virus (HBV) produces HBV and induces humoral immune response in mice. *Biochem Biophys Res Commun*. 2003; 300(3):784–788.
29. Eguchi T, et al. Regulatory mechanism of human connective tissue growth factor (CTGF/Hcs24) gene expression in a human chondrocytic cell line, HCS-2/8. *J Biochem*. 2001;130(1):79–87.
30. Cicha I, Goppelt-Struebe M. Connective tissue growth factor: context-dependent functions and mechanisms of regulation. *Biofactors*. 2009; 35(2):200–208.
31. Dews M, et al. Augmentation of tumor angiogenesis by a Myc-activated microRNA cluster. *Nat Genet*. 2006; 38(9):1060–1065.
32. Ernst A, et al. De-repression of CTGF via the miR-17-92 cluster upon differentiation of human glioblastoma spheroid cultures. *Oncogene*. 2010; 29(23):3411–3422.
33. Tanzer A, Stadler PF. Molecular evolution of a microRNA cluster. *J Mol Biol*. 2004;339(2):327–335.
34. Montes de Oca Luna R, Wagner DS, Lozano G. Rescue of early embryonic lethality in mdm2-deficient mice by deletion of p53. *Nature*. 1995; 378(6553):203–206.
35. Xiong S, Van Pelt CS, Elizondo-Fraire AC, Liu G, Lozano G. Synergistic roles of Mdm2 and Mdm4 for p53 inhibition in central nervous system development. *Proc Natl Acad Sci U S A*. 2006;103(9):3226–3231.
36. Hikita H, et al. Mcl-1 and Bcl-xL cooperatively maintain integrity of hepatocytes in developing and adult murine liver. *Hepatology*. 2009;50(4):1217–1226.
37. Brigstock DR. The connective tissue growth factor/cysteine-rich 61/nephroblastoma overexpressed (CCN) family. *Endocr Rev*. 1999;20(2):189–206.
38. Gao R, Brigstock DR. A novel integrin alpha5beta1 binding domain in module 4 of connective tissue growth factor (CCN2/CTGF) promotes adhesion and migration of activated pancreatic stellate cells. *Gut*. 2006;55(6):856–862.
39. Song JJ, et al. Connective tissue growth factor (CTGF) acts as a downstream mediator of TGF-beta1 to induce mesenchymal cell condensation. *J Cell Physiol*. 2007;210(2):398–410.
40. Abou-Shady M, et al. Connective tissue growth factor in human liver cirrhosis. *Liver*. 2000;20(4):296–304.
41. Hora C, et al. Connective tissue growth factor, steatosis and fibrosis in patients with chronic hepatitis C. *Liver Int*. 2008;28(3):370–376.
42. Williams EJ, Gaca MD, Brigstock DR, Arthur MJ, Benyon RC. Increased expression of connective tissue growth factor in fibrotic human liver and in activated hepatic stellate cells. *J Hepatol*. 2000;32(5):754–761.
43. Paradis V, et al. High glucose and hyperinsulinemia stimulate connective tissue growth factor expression: a potential mechanism involved in progression to fibrosis in nonalcoholic steatohepatitis. *Hepatology*. 2001;34(4 pt 1):738–744.
44. George J, Tsutsumi M. siRNA-mediated knockdown of connective tissue growth factor prevents N-nitrosodimethylamine-induced hepatic fibrosis in rats. *Gene Ther*. 2007;14(10):790–803.
45. Li G, et al. Inhibition of connective tissue growth factor by siRNA prevents liver fibrosis in rats. *J Gene Med*. 2006;8(7):889–900.
46. Paradis V, et al. Expression of connective tissue growth factor in experimental rat and human liver fibrosis. *Hepatology*. 1999;30(4):968–976.
47. Gressner OA, Lahme B, Demirci I, Gressner AM, Weiskirchen R. Differential effects of TGF-beta on connective tissue growth factor (CTGF/CCN2) expression in hepatic stellate cells and hepatocytes. *J Hepatol*. 2007;47(5):699–710.
48. Weng HL, et al. Profibrogenic transforming growth factor-beta/activin receptor-like kinase 5 signaling via connective tissue growth factor expression in hepatocytes. *Hepatology*. 2007;46(4):1257–1270.
49. Tong Z, Chen R, Alt DS, Kemper S, Perbal B, Brigstock DR. Susceptibility to liver fibrosis in mice expressing a connective tissue growth factor transgene in hepatocytes. *Hepatology*. 2009;50(3):939–947.
50. Canbay A, Taimr P, Torok N, Higuchi H, Friedman S, Gores GJ. Apoptotic body engulfment by a human stellate cell line is profibrogenic. *Lab Invest*. 2003;83(5):655–663.
51. Ku JL, et al. Establishment and characterisation of six human biliary tract cancer cell lines. *Br J Cancer*. 2002;87(2):187–193.
52. Ohgawara T, et al. Regulation of chondrocytic phenotype by micro RNA 18a: involvement of Ccn2/Ctgf as a major target gene. *FEBS Lett*. 2009; 583(6):1006–1010.
53. Duisters RF, et al. miR-133 and miR-30 regulate connective tissue growth factor: implications for a role of microRNAs in myocardial matrix remodeling. *Circ Res*. 2009;104(2):170–178.
54. Yan HL, et al. Repression of the miR-17-92 cluster by p53 has an important function in hypoxia-induced apoptosis. *EMBO J*. 2009;28(18):2719–2732.
55. Komarov PG, et al. A chemical inhibitor of p53 that protects mice from the side effects of cancer therapy. *Science*. 1999;285(5434):1733–1737.
56. Ostrau C, et al. Lovastatin attenuates ionizing radiation-induced normal tissue damage in vivo. *Radiother Oncol*. 2009;92(3):492–499.
57. Vozenin-Brotons MC, et al. Fibrogenic signals in patients with radiation enteritis are associated with increased connective tissue growth factor expression. *Int J Radiat Oncol Biol Phys*. 2003;56(2):561–572.
58. Haydont V, Riser BL, Aigueperse J, Vozenin-Brotons MC. Specific signals involved in the long-term maintenance of radiation-induced fibrogenic differentiation: a role for CCN2 and low concentration of TGF-beta1. *Am J Physiol Cell Physiol*. 2008;294(6):C1332–C1341.
59. Kodama T, et al. Thrombocytopenia exacerbates cholestasis-induced liver fibrosis in mice. *Gastroenterology*. 2010;138(7):2487–2498.
60. Itahana K, Campisi J, Dimri GP. Methods to detect biomarkers of cellular senescence: the senescence-associated beta-galactosidase assay. *Methods Mol Biol*. 2007;371:21–31.
61. Kodama T, et al. BH3-only activator proteins, Bid and Bim, are dispensable for Bak/Bax-dependent thrombocyte apoptosis induced by Bcl-xL deficiency: molecular requisites for the mitochondrial pathway to apoptosis in platelets. *J Biol Chem*. 2011;286(16):13905–13913.

Cancer Immunol Immunother (2011) 60:1565–1575
DOI 10.1007/s00262-011-1051-1

ORIGINAL ARTICLE

Comprehensive immunological analyses of colorectal cancer patients in the phase I/II study of quickly matured dendritic cell vaccine pulsed with carcinoembryonic antigen peptide

Mitsuru Sakakibara · Tatsuya Kanto · Michiyo Hayakawa · Shoko Kuroda · Hideki Miyatake · Ichiyo Itose · Masanori Miyazaki · Naruyasu Kakita · Koyo Higashitani · Tokuhiro Matsubara · Naoki Hiramatsu · Akinori Kasahara · Tetsuo Takehara · Norio Hayashi

Received: 8 March 2011 / Accepted: 24 May 2011 / Published online: 17 June 2011

Abstract Dendritic cell (DC) vaccine has been used to treat patients with advanced colorectal cancer (CRC). The results of vaccine-induced clinical responses have not always been satisfactory partially because of DC incompetence. In order to evaluate the feasibility of novel mature DCs for therapeutic adjuvants against CRC, we conducted clinical trials with carcinoembryonic antigen (CEA) peptide-loaded DC quickly generated with a combination of OK432 (Streptococcuspyogenes preparation), prostanoid, and interferon-α (OPA-DC). In the ten patients enrolled in this study, the OPA-DC vaccine was well tolerated and administered four times every 2 weeks except for two patients, who were switched to other treatments due to disease progression. Among the eight evaluable patients, one displayed stable disease (SD), while the remaining seven showed progressive disease (PD). In the SD patient, natural killer (NK) cell frequency and cytolytic activity were increased. In the same patient, the frequency of CEA-specific cytotoxic T cells (CTLs) increased stepwise with repetitive vaccinations; however, most of the CTLs exhibited central memory phenotype. In those with PD, NK cells proliferated well regardless of failure of response, whereas CTLs failed to do so. We concluded that the OPA-DC vaccine is well tolerated and has immune-stimulatory capacity in patients with CRC. Additional modulation is needed to attain significant clinical impact.

Keywords Dendritic cell · Vaccine · Cancer · Clinical study

Electronic supplementary material The online version of this article (doi:10.1007/s00262-011-1051-1) contains supplementary material, which is available to authorized users.

M. Sakakibara · T. Kanto (✉) · M. Hayakawa · M. Miyazaki · N. Kakita · K. Higashitani · T. Matsubara · N. Hiramatsu · T. Takehara
Department of Gastroenterology and Hepatology, Osaka University Graduate School of Medicine, 2-2 Yamadaoka, Suita, Osaka 565-0871, Japan
e-mail: kantot@gh.med.osaka-u.ac.jp

T. Kanto · S. Kuroda
Department of Dendritic Cell Biology and Clinical Applications, Osaka University Graduate School of Medicine, 2-2 Yamadaoka, Suita, Osaka 565-0871, Japan

H. Miyatake
Osaka Police Hospital, Osaka, Japan

I. Itose · N. Hayashi
Kansai Rosai Hospital, Hyogo, Japan

A. Kasahara
Department of General Medicine, Osaka University Graduate School of Medicine, 2-2 Yamadaoka, Suita, Osaka 565-0871, Japan

Introduction

Colorectal cancer (CRC) is one of the most intractable malignant diseases causing the death of 600 thousand people annually around the world. Recently, the development of new chemotherapeutic regimens including molecular-targeted drugs has significantly improved the clinical outcomes of patients with CRC [1]. However, the severe adverse effects of chemotherapeutic agents often deteriorate their quality of life (QOL), thus limiting continuation of therapy at full dose. The development of better therapies against CRC is needed.

Dendritic cells (DCs) are the most potent antigen-presenting cells that enhance innate and adaptive immune reactions. Previous studies have demonstrated that antigen-loaded DC is one of the most promising candidates for a

therapeutic vaccine to induce tumor-specific immune reactions and preferable clinical responses in cancer patients with limited side effects. However, less than 10% of vaccinated patients showed favorable clinical responses [2, 3]. One of the primary reasons for such unsatisfactory results may be that the DCs have not been fully exploited to induce anti-tumor immunity.

Previous DC-vaccine studies have shown that mature DCs are better than immature ones for inducing anti-tumor responses in patients. The protocols of maturation stimuli are yet to be standardized. Although a combination stimulus using interleukin (IL)-1β, IL-6, tumor necrosis factor (TNF)-α, and prostaglandin (PG)-E2 is widely used as a monocyte-conditioned medium (MCM) mimic for monocyte-derived DCs (MoDCs), it lacks the ability to promote DCs to secrete IL-12p70 [4], a well-known enhancer of cytotoxic activity of natural killer (NK) cells and cytotoxic T lymphocytes (CTLs) [5, 6]. From the mechanistic point of view, DCs loaded with antigens migrate into draining lymph nodes, where they produce IL-12p70 and activate NK cells, prime type-1 helper-T (Th1) cells and CTLs [7, 8]. We have previously reported that novel mature DCs (OPA-DCs) more effectively exert such functions than MCM-mimic DCs, which can be generated even from monocytes of refractory cancer patients within 3 days by using a combination of OK432 (Streptococcus pyogenes preparation), low-dose prostanoid, and interferon (IFN)-α [9] (OPA). In order to evaluate the tolerability and the clinical or immunological responses of OPA-DC vaccine, we conducted a phase I/II clinical study of OPA-DC vaccine in patients with CRC, which shed light on the importance of NK cells and the limitations of CTL differentiation even with fully matured DC.

Table 1 Eligibility criteria for the enrollment of patients with colorectal cancer for receiving quickly matured dendritic cell vaccine

(1) Eligibility criteria	(a) Patients with colon cancer (stage IV)
	(b) Performance status: 0–2
	(c) Age: 20–75 years
	(d) Tolerability for apheresis
	(e) Stability in bone marrow, liver, and renal functions:
	2,000 < WBC (/μl) < 15,000, Plt (/μl) > 75,000, AST and ALT (IU/l) < 150, T-bil (mg/dl) < 2.0, Crn < 2.0
	(f) Acquired informed consent
	(g) Having metastatic lesions for the assessment of therapeutic efficacy
	(h) More than 4 weeks have passed from previous anti-cancer treatments
	(i) HLA-A*2402 positive
	(j) Increased serum CEA level: >5 ng/ml
	(k) Positivity for CEA in cancer tissues
(2) Exclusion criteria	(a) Pregnant or lactating woman
	(b) Severe bleeding tendency: PT < 50%, APTT > 60 s, fibrinogen < 100 mg/dl, FDP > 20 μg/ml
	(c) Patient with infectious diseases (HIV, HBV, HCV, HTLV, RPR)
	(e) Patient with autoimmune disorders
	(f) Patient who needs to take steroids or immunosuppressive drugs during treatment
	(g) Patient who has uncontrollable metastatic brain or intrathecal tumors
	(h) Patient whom the doctors define as inappropriate

Subjects and methods

Subjects

Patients with advanced CRC (stage IV) who had been followed in or referred to Osaka University Hospital were enrolled as candidates in this clinical trial. The eligibility and exclusion criteria are summarized in Table 1. Among them, ten patients were selected. Their clinical backgrounds are given in Table 2.

Study design

The current clinical trial was performed to evaluate tolerability as well as immune and clinical responses; it has been registered with the University-hospital Medical Information Network Clinical Trials Registry (UMIN-CTR), under the code of UMIN000000743. The protocol was approved by the ethical committee of the Osaka University Graduate School of Medicine and also reviewed by the Translational Research Review Board, Osaka University Hospital. Standard operating procedures for manufacturing OPA-DCs were reviewed by the Medical center for Translational Research (MTR). Every detailed procedure described in the Manufacturing Instructions and Records was programmed to automatic process-control software to avoid operational errors. All patients gave written informed consent prior to the treatment.

The patients were vaccinated four times every 2 weeks in conformity with the regulation in previous DC vaccine [10–12]. In order to collect peripheral blood mononuclear cells (PBMCs) as a DC source, they underwent leukocyte apheresis at the first day of each session. After OPA-DCs had been generated as described in the next paragraph, they were administered subcutaneously at bilateral groin sites. Blood samples were collected before and 2 weeks after DC injection for the purpose of immunological and biochemical tests. Serum carcinoembryonic antigen (CEA) levels were determined on the day of blood collection. Two

Table 2 Clinical characteristics and outcomes of ten patients enrolled in this study

Case	Gender	Age	Metastases	CEA (ng/ml)[a]	Total tumor volume (cm^3)[a]	Administrated DCs (mean) ($\times 10^6$/injection)	DC injection time	CEA decline	RECIST
1	Female	62	Lung	111	4.7	106.7	8	+	SD
2	Female	64	Lung, liver	647	590.8	11.2	4	–	PD
3	Female	63	Lung, liver	987	603.3	19.2	4	–	PD
4	Male	60	Lung, liver	631	694.4	121.1	4	–	PD
5	Female	48	Lung, liver, peritoneal dissemination	482	Difficult to measure[b]	Withdrawn	2	Withdrawn	
6	Male	65	Liver	925	64.7	51.6	4	+	PD
7	Female	59	Liver, pancreas	692	543.7	115.0	4	–	PD
8	Female	42	Lung, liver	12	110.0	36.6	4	–	PD
9	Female	32	Lung, liver, abdominal wall, LN	402	163.7	Withdrawn	2	Withdrawn	
10	Male	49	Lung, abdominal LN	612	19.1	35.225	4	–	PD

[a] Before vaccination

[b] Peritoneal disseminations are too small to measure their diameter

weeks after the last vaccination, the clinical response was evaluated by the changes in tumor size measured on computerized tomography (CT) scans, based on the Response-Evaluation Criteria In Solid Tumors (RECIST) [13]. Toxicity was scored occasionally according to the National Cancer Institute Common Terminology Criteria for Adverse Events (NCI-CTCAE) v. 3.0. If severe toxicities of grade 3 or 4 developed, the patient was withdrawn from the study and switched to other appropriate treatment. A successive series of vaccinations could be applied to the patients evaluated as achieving a partial response (PR) or a stable disease (SD) condition based on the RECIST criteria.

Preparation of quickly inducible mature dendritic cells (OPA-DCs)

The OPA-DCs were generated as reported previously with some modifications [9]. At least 5×10^8 PBMCs were recovered via leukapheresis (Amicus) (Baxter, Deerfield, IL) from the patients. The PBMCs were incubated at a concentration of at least 5×10^6 cells/ml with serum-free AIM-V in 225 cm^2 culture flasks (Iwaki, Japan) for 2–3 h at 37°C in 5% CO_2. Subsequently, these flasks were washed with saline in order to separate monocytes by means of their preferential adherence to plastic [9]. Briefly, monocytes were cultured with 50 ng/ml GM-CSF and 20 ng/ml IL-4 for 3 days at 37°C in 5% CO_2. During the final 24 h, the cells were matured with 0.1 KE/ml OK432, 500 IU/ml IFN-α, and 50 ng/ml PG-E1. Concomitantly, 20 μg/ml CEA.652(9) was loaded to the cells. On day 3 of culture, non-adherent cells (OPA-DCs) were harvested. These procedures were performed in the cell-processing center affiliated with MTR under a clean condition according to the guidelines for translational research using human stem cells by Japanese Ministry of Health, Welfare and Labor.

Quality assessment of DC injections

During the DC-preparation process, samples of the culture supernatant were collected. No bacterial contamination was confirmed by means of their endotoxin measurement. Before handling the OPA-DC injections, we examined their viability and cell number using 0.3% trypan-blue staining. Viability was assessed as the percentage of viable cells among all countable cells. All the final products were confirmed as having at least 70% viability and containing at least 3.0×10^6 viable cells in conformity with the regulation in previous DC vaccine [10–12]. The purity of DCs was also examined. Briefly, the cells sampled from each final product were stained with fluorescent-material-conjugated anti-CD14 monoclonal antibody (mAb), anti-CD11c mAb, and anti-HLA-DR mAb. They were analyzed on a FACS Caliber (BD, Franklin Lakes, NJ). The live cells, except for lymphoid cells, were gated at forward scatter versus side scatter plot. Subsequently, the percentage of the CD14-/CD11c+/HLA-DR+ cells among the gated cells was analyzed as the purity. All final products were confirmed as having at least 70% purity.

Reagents

Recombinant human granulocyte–macrophage colony-stimulating factor (GM-CSF) and IL-4 were purchased from Primmune Inc., Japan. OK432 (Picibanil®) was purchased from Chugai, Japan. The amount of OK432 is expressed in units designated as KE (Klinische Einheit

[clinical unit]). One KE OK432 is equivalent to 0.1 mg dry streptococci. Natural human IFN-α (OIF®) was purchased from Otsuka, Japan. PG-E1 (Prostandin®) was purchased from Ono, Japan. The 9-mer peptide (CEA.652(9): TYACFVSNL), reported to be a human leukocyte antigen (HLA)-A*2402 restricted CTL epitope in CEA [9], was purchased from TaKaRa Bio (Japan) or Mimotope-Genzyme Pharmaceuticals (Switzerland). Therapeutic grade medium (AIM-V) was purchased from Invitrogen (Carlsbad, CA).

Fluorescent antibodies and HLA/peptide-pentamer

Fluorescein-isothiocyanate (FITC)-conjugated Lineage-Cocktail 1, anti-CD14 mAb (M5E2), anti-CD3 mAb (UCHT1), anti-CD4 mAb (RPA-T4), anti-CD27 mAb (M-T271), and anti-CD45RO mAb (UCHL1) were purchased from Becton–Dickinson (BD), Franklin Lakes, NJ. FITC-conjugated anti-CCR7 mAb (150503) was purchased from R&D Systems, McKinley Place, NE. Phycoerythrin (PE)-conjugated anti-CCR4 mAb (1G1), anti-CD4 mAb (RPA-T4), anti-CD45RA mAb (HI100), and anti-CD69 mAb (FN50) were obtained from BD. PE-conjugated anti-FoxP3 mAb (PCH101) was obtained from eBiosciences, San Diego, CA. PE-conjugated anti-CXCR3 mAb (49801) was purchased from R&D Systems. Peridinin-chlorophyll-protein-complex (PerCP)-conjugated anti-CD4 mAb (SK3), anti-CD8 mAb (SK1), and anti-HLA-DR mAb were purchased from BD. Allophycocyanin (APC)-conjugated anti-CD11c mAb (B-ly6) and anti-CD56 mAb (B159) were obtained from BD. APC-conjugated anti-CD4 mAb (13B8.2) was purchased from Beckman Coulter Inc., Fullerton, CA. PE-conjugated HLA-A*2402/CEA.652(9)-pentamer (CEA(24)-pentamer) and HLA-A*2402/EBV peptide (HLA-A*2402 restricted peptide derived from Epstein-Bar virus (EBV) LMP2: TYGPVFMSL)-pentamer were purchased from ProImmune Ltd., Bradenton, FL.

Cell lines

The NK-cell-sensitive cell line (K562) was obtained from ATCC (Manassas, VA). T2-A24 is a transporter associated with an antigen processing (TAP) deficient cell line (T2) transfected with HLA-A*2402 gene. This cell line expresses a high level of HLA-A24 protein and is used for targets in cytotoxicity assay. K562 and T2-A24 were cultured in RPMI-1640 containing 10% fetal calf serum (FCS), 100 IU/ml penicillin, and 100 μg/ml streptomycin at 37°C in 5% CO_2.

Calculation of total tumor volume

We calculated the total tumor volume of each patient before vaccination. Maximum diameters (D_1, D_2, ...) were measured for all visible tumors in CT images from the neck to the perineum, and total tumor volume was calculated as follows:

$$\text{Total Tumor Volume} = 3.14 \times \left(D_1^3 + D_2^3 + \ldots\right)/6.$$

Assessment of immune responses

(1) Frequency analyses of immune cells

PBMCs derived from blood samples were stained with fluorescent-material conjugated antibodies or a CEA(24)-pentamer. We analyzed the frequency of NK, Th1, Th2, FoxP3+ regulatory CD4+ T cells (Treg), and CEA.652(9)-specific CTLs on a FACS canto II (BD). For the analysis of Tregs, the cells were permeabilized with the Human FoxP3 Buffer Set (BD). Th1 and Th2 cells were detected as CD4+/CD45RO+/CXCR3+ and CD4+/CD45RO+/CCR4+ cells, respectively [14]. NK cells were characterized as CD3−/CD56+ cells and their active phenotypes were assessed by the expression of CD69. The ratios of CD69+ NK-cell frequency before and 2 weeks after every DC injection were calculated as the CD69+ NK variation rate (VR). We analyzed FoxP3+ Tregs as CD4+/CD45RO+/$CD25^{high}$/Foxp3+ cells. Highly avid CTLs for CEA.652(9) were identified as CD8+/CEA(24)-pentamer+ cells. Additionally, the CTLs were subdivided into CCR7+/CD45RA- central memory cells, CCR7−/CD4RA− effector memory cells, and CCR7−/CD45RA+ terminal differentiated effector memory cells [15].

(2) Analysis of NK cell activity

The cytotoxic ability of NK cells during vaccination was analyzed by flow-cytometric methods [16]. NK cells were separated from PBMCs using CD56 microbeads (Miltenyi Biotec). K562 cells were labeled with carboxyfluorescein succinimidyl ester (Invitrogen) and cultured with or without NK cells in 24-well culture plates (Falcon) for 12 h at 37°C in 5% CO_2 (E/T ratio: 24/1). At the end of the incubation, the samples were put on ice and 50 μg/ml propidium iodide (SIGMA) was added for DNA labeling of the dead cells. The samples were then incubated for 10 min on ice and analyzed within 60 min using FACS Canto II (BD). The percentage of specific-target-cell death (cytotoxicity) was calculated as:

$$\text{cytotoxicity}(\%) = \frac{\text{dead targets in the sample}(\%) - \text{spontaneously dead targets}(\%)}{100 - \text{spontaneously dead targets}(\%)} \times 100$$

The representative plots of flow-cytometric analyses are given in Online Resource 1.

Statistical analysis

For the vaccinated patients, a comparison was made between plasma cytokine level and total tumor volume

before vaccination using the Pearson's product-moment correlation coefficient (r), which was analyzed with Prism 5 software (Graph Pad Software, San Diego, CA). A P value is the probability that an r value is zero. Therefore, a P value of less than 0.05 indicates that the two variables are correlated.

Results

Quality of the OPA-DC vaccine

The mean DC number administered at each vaccination is shown in Table 2. The viability and purity of DC from all patients were 91.1 ± 2.6% (mean ± SD) and 88.8 ± 4.28%, respectively. All products met the quality assessment of the OPA-DC vaccine except for one form Case 3 due to its lesser number.

Clinical outcomes

Eight of the ten patients enrolled in this study were able to receive at least one series of vaccinations. Two patients (Case 5 and 9) were withdrawn from the study because of ileus, respiratory distress, or obstructive jaundice of grade 3 accompanied by cancer progression. One patient (Case 1) displayed a clinical response of SD lasting 2 months from the initiation of vaccination. Two weeks after the first session, the diameter of the patient's maximum lung metastasis increased by less than 20% and cavity formation was observed at the core of the lesion (Fig. 1a). Based on such clinical responses to the first session, this patient received the second series of vaccinations. Seven other patients had PD after the therapy.

Decline in the serum CEA level during the vaccination period was observed in two patients (Case 1 and 6) (Fig. 1b). They had clearly smaller total tumor volumes in the body before vaccination than the other patients (Fig. 2).

Immunological responses

We previously reported that OPA-DC has potent Th1 priming ability in vitro [9]. Therefore, we analyzed the frequency of peripheral Th1 and Th2 cells during the vaccination period (Fig. 3a). In Cases 1 and 8, the Th1/Th2 ratio remained high during vaccination compared with the pre-vaccination value. In Case 1, the patient with SD continued to show increment of the Th1/Th2 ratio after vaccination during the two series of sessions.

OPA-DCs have potent ability to activate NK cells and antigen-specific CTLs in vitro [9]. Therefore, we analyzed the frequency of NK cells before and during vaccination (Fig. 3b). In all except Cases 2 and 10, the mean frequency of NK cells during vaccination increased compared with the pre-vaccination value. Moreover, in Cases 1 and 6 demonstrating a CEA decline, the NK cells displayed strong lytic activity against K562 cells after vaccination (Fig. 3c).

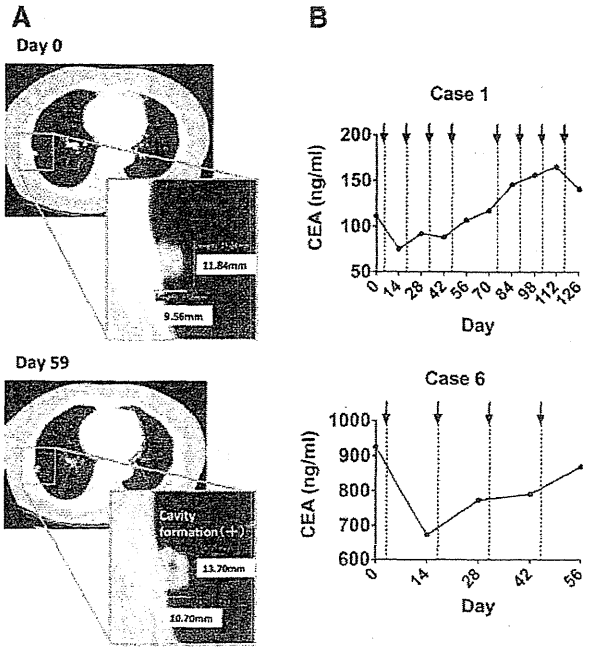

Fig. 1 Changes in CT images of metastatic lesion and serum CEA levels in patients after receiving the OPA-DC vaccines. **a** CT images of the patient with stable disease after OPA-DC vaccination (Case 1) are shown. The diameters of the maximum metastatic lesion in the lung are shown before (day 0) and after (day 59) the vaccination period. **b** The changes in serum CEA levels during vaccine treatment in the patients (Case 1 and 6) are shown. *Downward arrows* indicate the time points of OPA-DCs injections

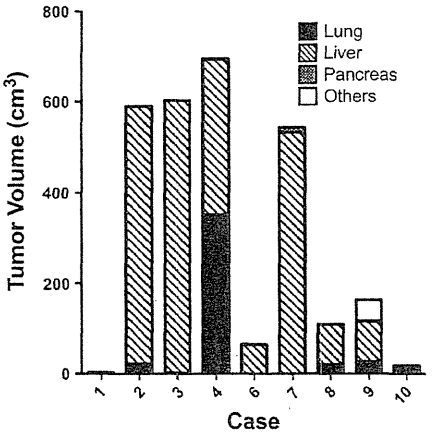

Fig. 2 Absence of correlation between total tumor volume and serum immunosuppressive cytokines in the vaccinated patients. Total tumor masses of each patient before vaccination were measured as described in "Subjects and methods". Localizations and volumes of metastatic tumors are shown

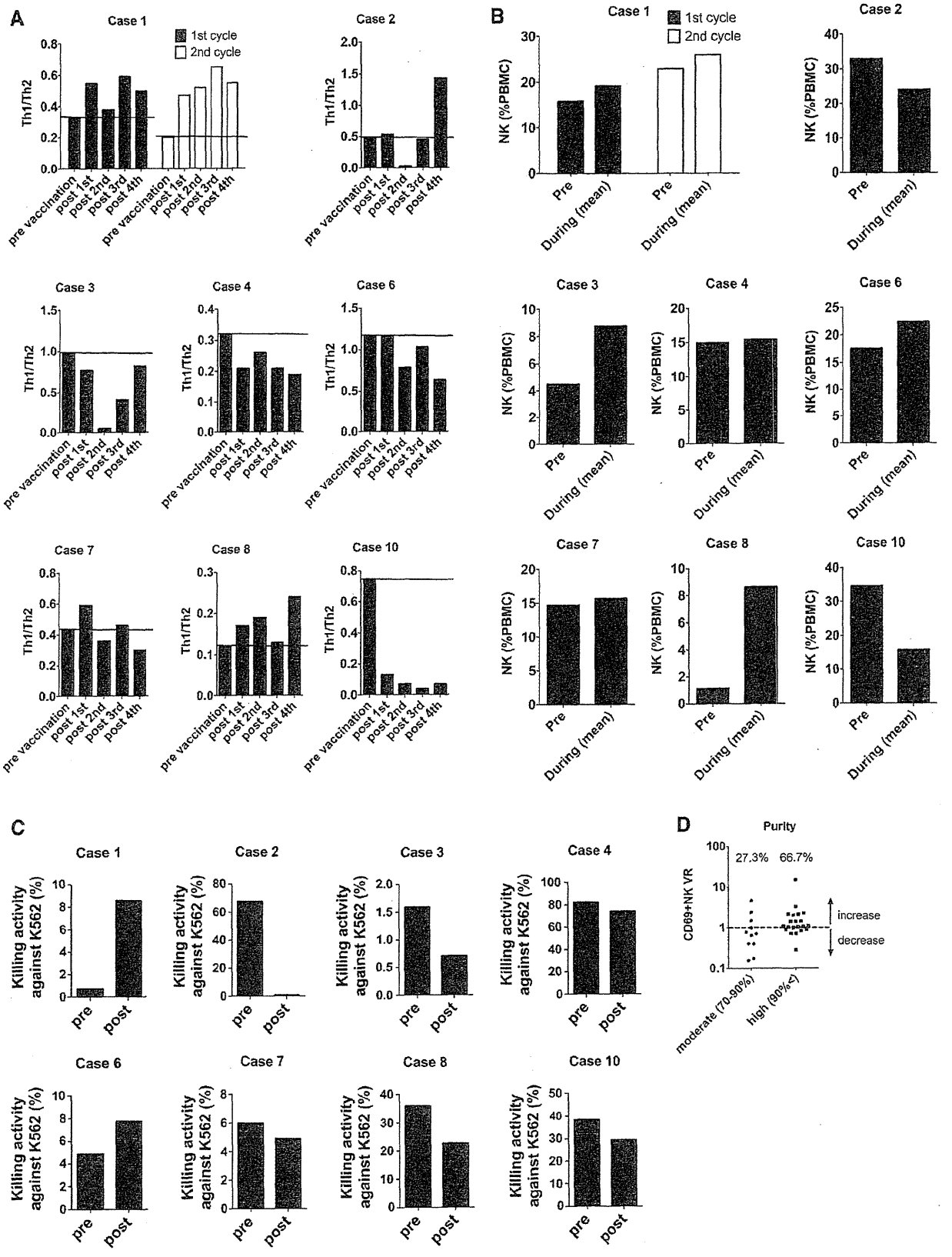
A
Case 1
1st cycle
2nd cycle
Th1/Th2
pre vaccination
post 1st
post 2nd
post 3rd
post 4th
Case 2
Case 3
Case 4
Case 6
Case 7
Case 8
Case 10
B
Case 1
1st cycle
2nd cycle
NK (%PBMC)
Pre
During (mean)
Case 2
Case 3
Case 4
Case 6
Case 7
Case 8
Case 10
C
Case 1
Killing activity against K562 (%)
pre
post
Case 2
Case 3
Case 4
Case 6
Case 7
Case 8
Case 10
D
Purity
27.3%
66.7%
CD69+NK VR
increase
decrease
moderate (70-90%)
high (90%<)

◀ **Fig. 3** Changes in Th1/Th2 ratio and NK cells before and during/after the OPA-DC vaccines. **a** Ratios between Th1 and Th2 frequency (Th1/Th2) were determined before and 2 weeks after every vaccination as described in "Subjects and methods". In Case 1, four additional injections of DCs were performed (*empty bars*). *Horizontal lines* in each graph indicate the Th1/Th2 value before vaccination. **b** NK cell frequency was examined before and during the vaccinations. The *values* are shown as the mean of the NK cell frequencies between the first and the last DC injections. **c** NK activities are evaluated by the killing of NK-sensitive K562 cells before and 2 weeks after the first DC injection. **d** CD69+ NK variation rates (VR) are shown for all DC injections of all patients in the first session. VR values above 1 mean that CD69+ NK cells increased with that single injection of DC. Percentages in the graphs depict the rate of CD69+ NK increment induced by DCs with quality

We and other investigators have found that DCs primed with OK432 can activate NK cells within 48 h [9, 17]. Such observations support the possibility of vaccine-dependent activation of NK cells with each DC injection. Therefore, we analyzed the increment of CD69 + NK cells after every DC injection with respect to its relationship with DC purity. In total, 32 injections were performed with eight patients in their first sessions. Among such vaccinations, 21 injections were done with highly pure DCs (purity: >90%) and the remaining 11 with moderately pure DCs (purity: 70–90%). As shown in Fig. 3d, regardless of the differences in clinical backgrounds of the patients, a post-vaccine increment of CD69 + NK cells was observed in 14 out of the 21 given highly pure DC injections (66.7%). In contrast, such an increment was detected only in 3 out of the 11 given moderately pure DC injections (27.3%). Therefore, highly pure DC injections resulted in a higher rate of NK activation compared with moderately pure DC injections.

Next, to assess the frequency of antigen-specific CTLs induced with OPA-DC vaccine, we analyzed PBMCs from vaccinated patients with CEA(24)-pentamer staining (Fig. 4a). In Case 1 with the SD response, the frequency of the pentamer-positive CTLs increased with vaccination. Of particular interest, during the second sessions, the frequency increased much more compared with those in the first sessions (Fig. 4a). In contrast, the frequency of specific CTLs against control peptide derived from Epstein-Bar virus (EBV) kept under 1% of all CD8+ T cells during all sessions (Online Resource 2). According to the differentiation stages, human CD8+ T cells have been subdivided into different populations based on their CD45RA and CCR7 expressions [15]. Therefore, we analyzed the frequencies of CEA.652(9)-specific central memory T (Tcm), effector memory T (Tem) and terminally differentiated Tem (Tem/td) cells during vaccination in Case 1 (Fig. 4b). The CEA.652(9)-specific Tcm cells increased gradually with OPA-DC vaccination; however, antigen-specific Tem or Tem/td cells were not induced. In other cases, including Case 6 with CEA decline, we did not observe such increment of antigen-specific CTLs after the vaccinations.

We performed ELISPOT assay in order to enumerate IFN-γ-producing CD8 cells reacting to the CEA peptide. Also, we had intended to measure the antigen-specific lytic activity of CTLs against CEA.652(9) pulsed T2-A24 cells by ^{51}Cr-releasing assay, but in all cases, no such responses were observed (data not shown).

Regulatory T cells (Treg) play an active role in the suppression of anti-tumor immune responses. Many investigators reported that the accumulation of Tregs is observed in various types of cancers including CRC [18–21]. Therefore, we analyzed the frequency of Tregs during vaccination. In Cases 2, 3, 6, and 7, Tregs decreased after the vaccinations (Fig. 5). It is noteworthy that in Case 6, the reduction in Tregs was maintained throughout the vaccination period. Delayed-type hypersensitivity (DTH) against CEA.652(9) peptide was not observed in any of the cases (data not shown).

Toxicity

All patients experienced grade-1 fever after every vaccination, but this could be controlled with anti-inflammatory drugs. In addition, induration of the vaccinated groin sites was observed about 2 weeks after the first vaccination with all patients. They were followed without treatment, except for one patient (Case 8) who received temporal antibiotics for abscess formation of the induration. OPA-DC vaccine could be performed without severe toxicity for all patients.

Discussion

Dendritic cells pulsed with CEA peptide are one of the feasible vaccines to induce anti-tumor immunity in patients with CRC [22]. We have previously reported that novel mature DCs (OPA-DCs) can be generated from monocytes using OK-432, low-dose prostanoid, and IFN-α (OPA) by a short-term process. OPA-DCs possess potent migrating ability and stimulating activity for Th1, CTL, and NK cells, which are desirable for DC vaccines using peptide antigen against cancers [9]. In this phase I/II clinical study, we evaluated the safety and efficacy of vaccination with OPA-DCs pulsed with CEA.652(9) peptide in ten patients with metastatic CRC. We chose the peptide as a target antigen because it has been reported as a tumor-associated antigen achieving preferable responses in previous cancer vaccine studies [23, 24]. OPA-DCs offer several advantages in clinical settings [25]. First, even with serum-free media, OPA-DCs are likely to possess better functional abilities with large-scale yield. Second, they can avoid the possibility of contamination and can save costs with the

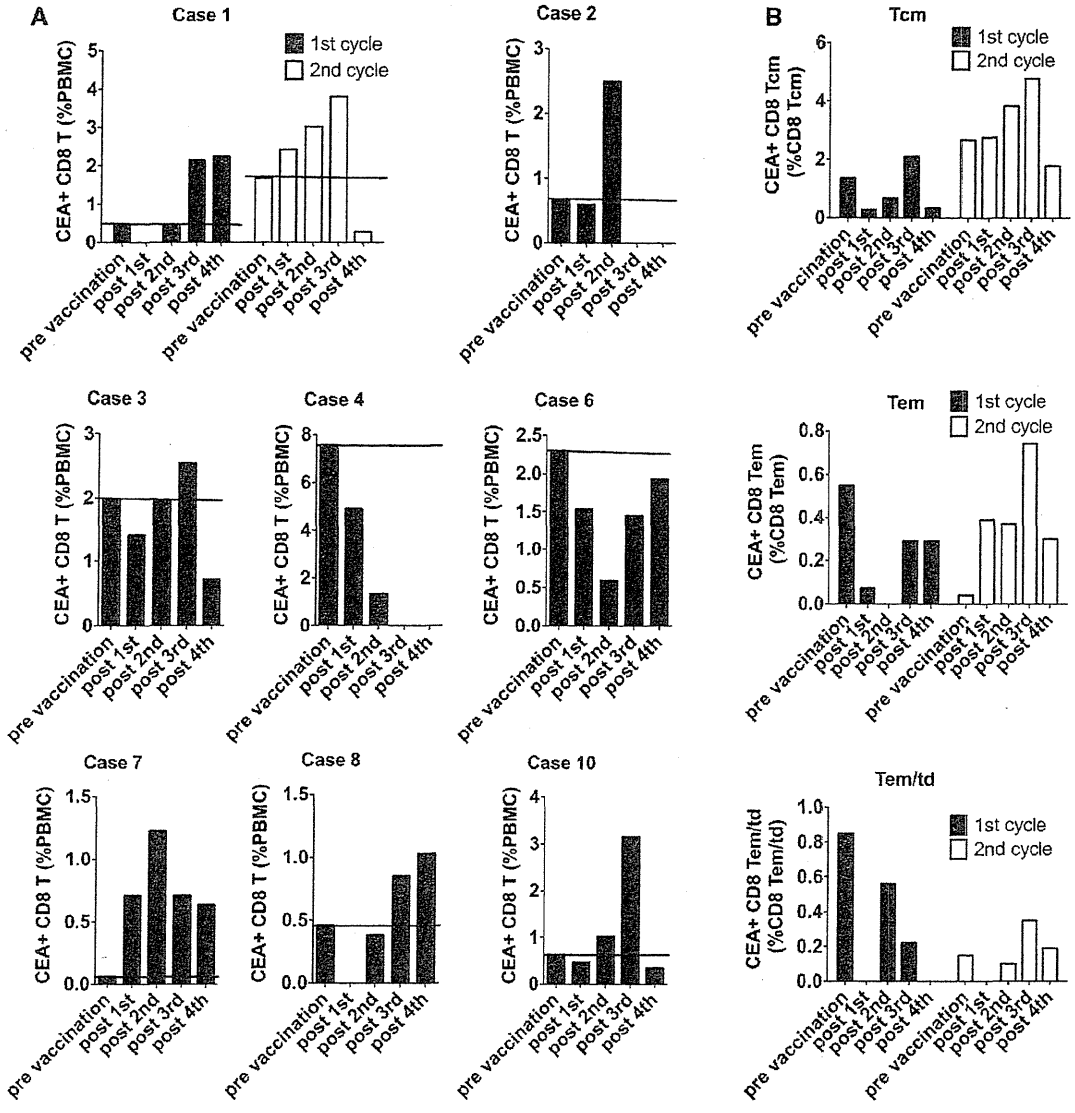

Fig. 4 Differentiation of CTLs was impaired regardless of the increased frequency of CEA-pentamer-positive CD8 T cells after DC vaccinations. **a** CEA-specific CTLs, as judged by CEA-pentamer-positive CD8+ T cells, were counted as described in "Subjects and methods". The *horizontal lines* in each graph indicate the frequency of CEA-pentamer-positive cells before vaccination. **b** In the patient who showed an SD response (Case 1), the frequency of CEA-pentamer-positive CD8+ central memory T cells (Tcm), effector memory T cells (Tem), and terminal differentiated effector memory T cells (Tem/td) was analyzed as described in "Subjects and methods"

generation of clinical-grade DCs. Alternate strategies using short-term cultured DCs have been reported elsewhere [26–28]; however, this is the first clinical study of anti-tumor vaccine using quickly generated DCs.

Regarding toxicity, the vaccination with OPA-DCs was well tolerated in patients with advanced CRC. The most common adverse events were grade-1 fever and indurations at the injection sites. Such toxicities were comparable to findings reported for previous DC-vaccine trials [29–32]. Two patients were withdrawn from the study because of grade-3 ileus, respiratory distress, or obstructive jaundice; however, these problems were caused by exacerbation of preexisting peritoneal disseminations, lymphangitic carcinomatosis, or liver metastases.

In this clinical study, we observed an SD response in one patient (Case 1). Interestingly, several tumor lesions in this patient formed a central cavity, which was probably attributed to immunological tumor necrosis triggered by the OPA-DC vaccine. Histological analysis could have offered support for this, but we could not perform biopsies of the lesions for ethical reasons. Instead, some immunological events that could have contributed to her clinical outcomes were observed in the peripheral blood during vaccination. First, Th1 cells were dominant over Th2 cells

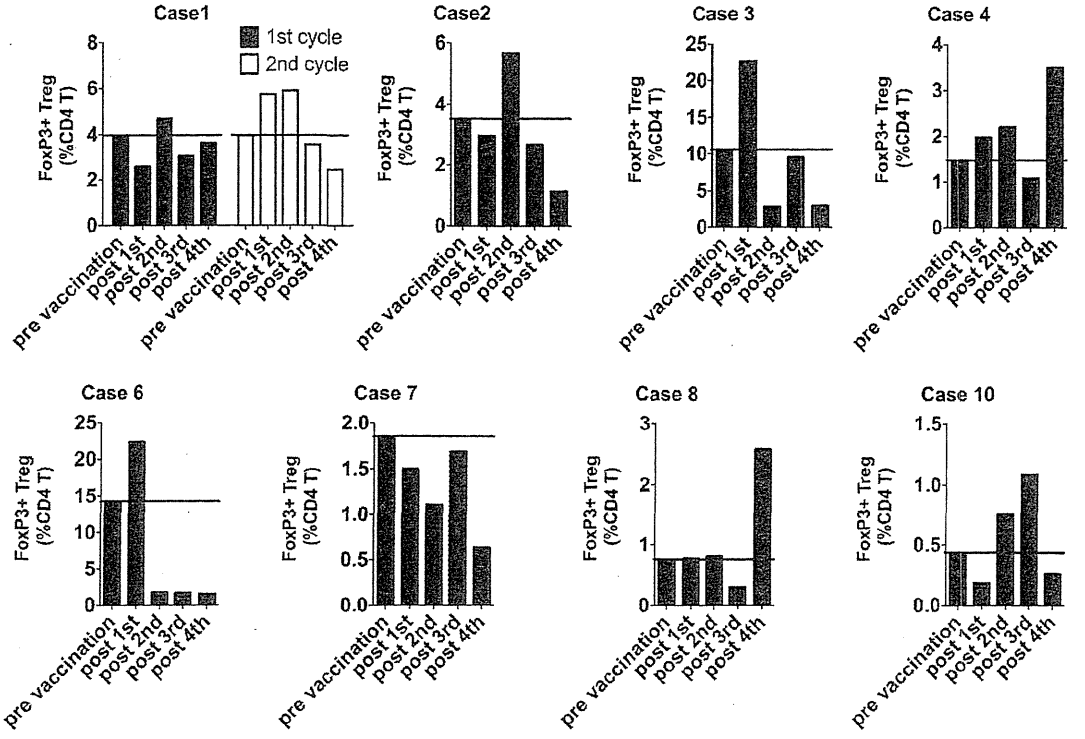

Fig. 5 Changes in FoxP3+ regulatory T cells varied during the OPA-DC vaccination period. Frequency of FoxP3+ CD4+ CD25+ T cells (depicted as Tregs) during the vaccination period is shown. *Horizontal lines* in each graph indicate the frequency of Tregs before vaccination

throughout her vaccination period. Second, NK cells had increased and were activated, and their in vitro lytic activity was enhanced after vaccination. In addition, specific CTLs that possess strong avidity to HLA-A*2402/CEA.652(9)-pentamer (CEA(24)-pentamer) were increased gradually with OPA-DC injections. These findings demonstrate that OPA-DCs can have significant immunological impact on patients even in refractory stages.

As for clinical outcomes, we observed decline in CEA in only 2 of 8 patients (Case 1 and 6) and stable disease in one (Case 1). Such results are comparable with those of previous reports regarding DC vaccine against CRC [31, 33, 34], which implies that additional modifications, other than highly active DC, are required to improve clinical responses with DC vaccine. In our study, the responders had lesser tumor volume than non-responders at the beginning of the vaccination period. In addition, regulatory T cells (Tregs) were reduced after OPA-DC vaccine in half of the treated patients. In a patient with CEA decline (Case 6), a sustained reduction in Tregs was observed throughout the vaccination period. It is not clear whether OPA-DCs directly reduce Tregs; however, Treg reduction may exert a favorable impact on the clinical outcome. Even if such inhibitory factors could be removed, a sizable number of cancer cells could not be completely eliminated by a limited number of effector cells educated by DC vaccine. Therefore, initiating vaccination at earlier stages of the disease could be a key to success for DC therapy.

Natural killer (NK) cells are potent anti-tumor effectors that reciprocally interact with DCs [35]. Many previous reports about DC vaccine have regarded CTLs as a principal effector providing anti-tumor immunity. However, there are few studies reporting NK cell activation in response to DC vaccine. Osada et al. [36] reported that NK number increased in 5 of 9 patients (55.6%) vaccinated with CEA-gene-transfected MoDCs, of which the clinical outcomes were correlated with NK activity rather than with T-cell responses. Our study showed that NK cell frequency was increased in 6 of 8 OPA-DC-vaccinated patients (75%). Such a high response rate shows that OPA-DCs possess potent ability to stimulate NK cells in vivo. In addition, our results showed that highly pure DC could activate NK cells compared with moderately pure one, which indicate that such NK activation is dependent on specific action of administrated DCs. Of interest, in two patients (Case 1 and 6), NK cells gained strong lytic activity after vaccination. Interestingly, only these two patients showed decline in serum CEA or a preferable clinical outcome as SD. In support of this possibility, Shimizu and Fujii [37] have reported that mice immunized with DC vaccine acquired "primed" NK cells, which could be quickly re-activated in response to tumor-cell challenge

even at 6–12 months after the vaccination. Such an observation suggests that NK cells primed with DC vaccine may contribute to long-term tumor rejection. Further exploration is needed to disclose how NK cells work in DC vaccine therapies.

In the patient displaying an SD response (Case 1), CEA(24)-pentamer-positive cells increased gradually with the injection of OPA-DCs. Interestingly, despite expansion of CTLs, we detected no IFN-γ-producing or antigen-specific-lytic ability of CTLs against antigen-loaded T2-A24 cells. One of the reasons for such a discrepancy may be the impaired differentiation of CTLs, exhibited by the predominance of Tcm phenotype as antigen-specific CTLs in this study. Sallusto et al. [15] identified different populations of memory CD8+ T cells in the peripheral blood of humans. The Tcm cells are reported to attain potent proliferative or IL-2-producing ability critical for maintenance of memory-T-cell pools, whereas Tem or Tem/td cells possess potent effector function such as IFN-γ/perforin production or cytotoxicity [15]. It is still uncertain which cells, Tcm or Tem, are more advantageous in providing protective immunity against cancer [38]. Mornarini et al. [39] reported that although most melanoma patients displayed antigen-specific CTLs belonging to Tcm subsets in tumor-invaded lymph nodes, few perforin-producing Tem or Tem/td cells infiltrated in the neoplastic tissues, and they found no evidence for tumor regression. Although the factors that regulate CTL differentiation are still unclear, further understanding of such regulators could provide clues to developing effective vaccines.

In summary, quickly inducible OPA-DC vaccine is tolerated and could induce preferable immunological responses in patients with advanced-stage CRC. OPA-DC vaccine exerted significant NK-activating ability, and such a response was partially linked to favorable clinical outcomes in the patients. Most antigen-specific CTLs induced with the OPA-DC vaccine belonged to a Tcm subset. In order to develop more practically effective DC vaccine against CRC, further investigation is necessary to explore the modality to induce coordinated and durable activation of both NK cells and CTLs.

Acknowledgments We are grateful to the members of MTR, especially to the following Drs. Toshiki Yoshimine (Director), Yoshiki Sawa (Director), Akira Myoui (Vice Director), ChunMan Lee, Junji Kawada, Haruki Ide, and Masao Umegaki (Project Managers).

References

1. Hwang J, Marshall JL (2006) Targeted therapy for colorectal cancer. Curr Opin Investig Drugs 7(12):1062–1066
2. de Vries IJM, Lesterhuis WJ, Scharenborg NM, Engelen LPH, Ruiter DJ, Gerritsen M-JP, Croockewit S, Britten CM, Torensma R, Adema GJ, Figdor CG, Punt CJA (2003) Maturation of dendritic cells is a prerequisite for inducing immune responses in advanced melanoma patients. Clin Cancer Res 9(14):5091–5100
3. Vilella R, Benítez D, Milà J, Lozano M, Vilana R, Pomes J, Tomas X, Costa J, Vilalta A, Malvehy J, Puig S, Mellado B, Martí R, Castel T (2004) Pilot study of treatment of biochemotherapy-refractory stage IV melanoma patients with autologous dendritic cells pulsed with a heterologous melanoma cell line lysate. Cancer Immunol Immunother 53(7):651–658. doi:10.1007/s00262-003-0495-3
4. Lee AW, Truong T, Bickham K, Fonteneau J-F, Larsson M, Da Silva I, Somersan S, Thomas EK, Bhardwaj N (2002) A clinical grade cocktail of cytokines and PGE2 results in uniform maturation of human monocyte-derived dendritic cells: implications for immunotherapy. Vaccine 20(Suppl 4):A8–A22
5. Mbawuike IN, Fujihashi K, DiFabio S, Kawabata S, McGhee JR, Couch RB, Kiyono H (1999) Human interleukin-12 enhances interferon-gamma-producing influenza-specific memory CD8+ cytotoxic T lymphocytes. J Infect Dis 180(5):1477–1486. doi:10.1086/315090
6. Alli RS, Khar A (2004) Interleukin-12 secreted by mature dendritic cells mediates activation of NK cell function. FEBS Lett 559(1–3):71–76. doi:10.1016/S0014-5793(04)00026-2
7. Dredge K, Marriott JB, Todryk SM, Dalgleish AG (2002) Adjuvants and the promotion of Th1-type cytokines in tumour immunotherapy. Cancer Immunol Immunother 51(10):521–531. doi:10.1007/s00262-002-0309-z
8. Toes RE, Offringa R, Feltkamp MC, Visseren MJ, Schoenberger SP, Melief CJ, Kast WM (1994) Tumor rejection antigens and tumor specific cytotoxic T lymphocytes. Behring Inst Mitt Jul(94):72–86
9. Sakakibara M, Kanto T, Inoue M, Kaimori A, Yakushijin T, Miyatake H, Itose I, Miyazaki M, Kuzushita N, Hiramatsu N, Takehara T, Kasahara A, Hayashi N (2006) Quick generation of fully mature dendritic cells from monocytes with OK432, low-dose prostanoid, and interferon-alpha as potent immune enhancers. J Immunother 29(1):67–77
10. Pandha HS, John RJ, Hutchinson J, James N, Whelan M, Corbishley C, Dalgleish AG (2004) Dendritic cell immunotherapy for urological cancers using cryopreserved allogeneic tumour lysate-pulsed cells: a phase I/II study. BJU Int 94(3):412–418. doi:10.1111/j.1464-410X.2004.04922.x
11. Babatz J, Röllig C, Löbel B, Folprecht G, Haack M, Günther H, Köhne C-H, Ehninger G, Schmitz M, Bornhäuser M (2006) Induction of cellular immune responses against carcinoembryonic antigen in patients with metastatic tumors after vaccination with altered peptide ligand-loaded dendritic cells. Cancer immunology, immunotherapy CII 55(3):268–276. doi:10.1007/s00262-005-0021-x
12. Liu K-J, Wang C–C, Chen L-T, Cheng A-L, Lin D-T, Wu Y-C, Yu W-L, Hung Y-M, Yang H-Y, Juang S-H, Whang-Peng J (2004) Generation of carcinoembryonic antigen (CEA)-specific T-cell responses in HLA-A*0201 and HLA-A*2402 late-stage colorectal cancer patients after vaccination with dendritic cells loaded with CEA peptides. Clin Cancer Res 10(8):2645–2651
13. Therasse P, Arbuck SG, Eisenhauer EA, Wanders J, Kaplan RS, Rubinstein L, Verweij J, Van Glabbeke M, van Oosterom AT, Christian MC, Gwyther SG (2000) New guidelines to evaluate the response to treatment in solid tumors. European Organization for Research and Treatment of Cancer, National Cancer Institute of the United States, National Cancer Institute of Canada. J Natl Cancer Inst 92(3):205–216
14. Syrbe U, Siveke J, Hamann A (1999) Th1/Th2 subsets: distinct differences in homing and chemokine receptor expression? Springer Semin Immunopathol 21(3):263–285
15. Sallusto F, Lenig D, Förster R, Lipp M, Lanzavecchia A (1999) Two subsets of memory T lymphocytes with distinct homing

potentials and effector functions. Nature 401(6754):708–712. doi:10.1038/44385
16. Marcusson-Stahl M, Cederbrant K (2003) A flow-cytometric NK-cytotoxicity assay adapted for use in rat repeated dose toxicity studies. Toxicology 193(3):269–279
17. West E, Morgan R, Scott K, Merrick A, Lubenko A, Pawson D, Selby P, Hatfield P, Prestwich R, Fraser S, Eves D, Anthoney A, Twelves C, Beirne D, Patel P, O'Donnell D, Watt S, Waller M, Dietz A, Robinson P, Melcher A (2009) Clinical grade OK432-activated dendritic cells: in vitro characterization and tracking during intralymphatic delivery. J Immunother 32(1):66–78. doi:10.1097/CJI.0b013e31818be071
18. Clarke SL, Betts GJ, Plant A, Wright KL, El-Shanawany TM, Harrop R, Torkington J, Rees BI, Williams GT, Gallimore AM, Godkin AJ (2006) CD4+ CD25+ FOXP3+ regulatory T cells suppress anti-tumor immune responses in patients with colorectal cancer. PLoS ONE 1:e129. doi:10.1371/journal.pone.0000129
19. Correale P, Rotundo MS, Del Vecchio MT, Remondo C, Migali C, Ginanneschi C, Tsang KY, Licchetta A, Mannucci S, Loiacono L, Tassone P, Francini G, Tagliaferri P (2010) Regulatory (FoxP3+) T-cell tumor infiltration is a favorable prognostic factor in advanced colon cancer patients undergoing chemo or chemoimmunotherapy. J Immunother 33(4):435–441. doi:10.1097/CJI.0b013e3181d32f01
20. Salama P, Phillips M, Grieu F, Morris M, Zeps N, Joseph D, Platell C, Iacopetta B (2009) Tumor-infiltrating FOXP3+ T regulatory cells show strong prognostic significance in colorectal cancer. J Clin Oncol 27(2):186–192. doi:10.1200/JCO.2008.18.7229
21. Wolf AM, Wolf D, Steurer M, Gastl G, Gunsilius E, Grubeck-Loebenstein B (2003) Increase of regulatory T cells in the peripheral blood of cancer patients. Clin Cancer Res 9(2):606–612
22. Lesterhuis WJ, De Vries IJ, Schreibelt G, Schuurhuis DH, Aarntzen EH, De Boer A, Scharenborg NM, Van De Rakt M, Hesselink EJ, Figdor CG, Adema GJ, Punt CJ (2010) Immunogenicity of dendritic cells pulsed with CEA peptide or transfected with CEA mRNA for vaccination of colorectal cancer patients. Anticancer Res 30(12):5091–5097
23. Ueda Y, Itoh T, Fuji N, Harada S, Fujiki H, Shimizu K, Shiozaki A, Iwamoto A, Shimizu T, Mazda O, Kimura T, Sonoda Y, Taniwaki M, Yamagishi H (2007) Successful induction of clinically competent dendritic cells from granulocyte colony-stimulating factor-mobilized monocytes for cancer vaccine therapy. Cancer Immunol Immunother CII 56(3):381–389. doi:10.1007/s00262-006-0197-8
24. Matsuda K, Tsunoda T, Tanaka H, Umano Y, Tanimura H, Nukaya I, Takesako K, Yamaue H (2004) Enhancement of cytotoxic T-lymphocyte responses in patients with gastrointestinal malignancies following vaccination with CEA peptide-pulsed dendritic cells. Cancer Immunol Immunother CII 53(7):609–616. doi:10.1007/s00262-003-0491-7
25. Koski GK, Cohen PA, Roses RE, Xu S, Czerniecki BJ (2008) Reengineering dendritic cell-based anti-cancer vaccines. Immunol Rev 222:256–276. doi:10.1111/j.1600-065X.2008.00617.x
26. Dauer M, Lam V, Arnold H, Junkmann J, Kiefl R, Bauer C, Schnurr M, Endres S, Eigler A (2008) Combined use of toll-like receptor agonists and prostaglandin E(2) in the FastDC model: rapid generation of human monocyte-derived dendritic cells capable of migration and IL-12p70 production. J Immunol Methods 337(2):97–105. doi:10.1016/j.jim.2008.07.003
27. Dauer M, Obermaier B, Herten J, Haerle C, Pohl K, Rothenfusser S, Schnurr M, Endres S, Eigler A (2003) Mature dendritic cells derived from human monocytes within 48 hours: a novel strategy for dendritic cell differentiation from blood precursors. J Immunol 170(8):4069–4076
28. Anguille S, Smits ELJM, Cools N, Goossens H, Berneman ZN, Van Tendeloo VFI (2009) Short-term cultured, interleukin-15 differentiated dendritic cells have potent immunostimulatory properties. J Transl Med 7:109. doi:10.1186/1479-5876-7-109
29. Avigan DE, Vasir B, George DJ, Oh WK, Atkins MB, McDermott DF, Kantoff PW, Figlin RA, Vasconcelles MJ, Xu Y, Kufe D, Bukowski RM (2007) Phase I/II study of vaccination with electrofused allogeneic dendritic cells/autologous tumor-derived cells in patients with stage IV renal cell carcinoma. J Immunother 30(7):749–761. doi:10.1097/CJI.0b013e3180de4ce8
30. Berntsen A, Trepiakas R, Wenandy L, Geertsen PF, thor Straten P, Andersen MH, Pedersen AE, Claesson MH, Lorentzen T, Johansen JS, Svane IM (2008) Therapeutic dendritic cell vaccination of patients with metastatic renal cell carcinoma: a clinical phase 1/2 trial. J Immunother 31(8):771–780. doi:10.1097/CJI.0b013e3181833818
31. Burgdorf SK, Fischer A, Myschetzky PS, Munksgaard SB, Zocca M-B, Claesson MH, Rosenberg J (2008) Clinical responses in patients with advanced colorectal cancer to a dendritic cell based vaccine. Oncol Rep 20(6):1305–1311
32. Trepiakas R, Berntsen A, Hadrup SR, Bjørn J, Geertsen PF, Straten PT, Andersen MH, Pedersen AE, Soleimani A, Lorentzen T, Johansen JS, Svane IM (2010) Vaccination with autologous dendritic cells pulsed with multiple tumor antigens for treatment of patients with malignant melanoma: results from a phase I/II trial. Cytotherapy. doi:10.3109/14653241003774045
33. Kavanagh B, Ko A, Venook A, Margolin K, Zeh H, Lotze M, Schillinger B, Liu W, Lu Y, Mitsky P, Schilling M, Bercovici N, Loudovaris M, Guillermo R, Lee SM, Bender J, Mills B, Fong L (2007) Vaccination of metastatic colorectal cancer patients with matured dendritic cells loaded with multiple major histocompatibility complex class I peptides. J Immunother 30(7):762–772. doi:10.1097/CJI.0b013e318133451c
34. Babatz J, Röllig C, Löbel B, Folprecht G, Haack M, Günther H, Köhne C-H, Ehninger G, Schmitz M, Bornhäuser M (2006) Induction of cellular immune responses against carcinoembryonic antigen in patients with metastatic tumors after vaccination with altered peptide ligand-loaded dendritic cells. Cancer Immunol Immunother 55(3):268–276. doi:10.1007/s00262-005-0021-x
35. Jinushi M, Takehara T, Kanto T, Tatsumi T, Groh V, Spies T, Miyagi T, Suzuki T, Sasaki Y, Hayashi N (2003) Critical role of MHC class I-related chain A and B expression on IFN-alpha-stimulated dendritic cells in NK cell activation: impairment in chronic hepatitis C virus infection. J Immunol 170(3):1249–1256
36. Osada T, Clay T, Hobeika A, Lyerly HK, Morse MA (2006) NK cell activation by dendritic cell vaccine: a mechanism of action for clinical activity. Cancer Immunol Immunother 55(9):1122–1131. doi:10.1007/s00262-005-0089-3
37. Shimizu K, Fujii S (2009) DC therapy induces long-term NK reactivity to tumors via host DC. Eur J Immunol 39(2):457–468. doi:10.1002/eji.200838794
38. Perret R, Ronchese F (2008) Memory T cells in cancer immunotherapy: which CD8 T-cell population provides the best protection against tumours? Tissue Antigens 72(3):187–194. doi:10.1111/j.1399-0039.2008.01088.x
39. Mortarini R, Piris A, Maurichi A, Molla A, Bersani I, Bono A, Bartoli C, Santinami M, Lombardo C, Ravagnani F, Cascinelli N, Parmiani G, Anichini A (2003) Lack of terminally differentiated tumor-specific CD8+ T cells at tumor site in spite of antitumor immunity to self-antigens in human metastatic melanoma. Cancer Res 63(10):2535–2545

Biochemical and Biophysical Research Communications 412 (2011) 92–97

Contents lists available at ScienceDirect

Biochemical and Biophysical Research Communications

journal homepage: www.elsevier.com/locate/ybbrc

Alterations in microRNA expression profile in HCV-infected hepatoma cells: Involvement of miR-491 in regulation of HCV replication via the PI3 kinase/Akt pathway

Hisashi Ishida [a], Tomohide Tatsumi [a], Atsushi Hosui [a], Takatoshi Nawa [a], Takahiro Kodama [a], Satoshi Shimizu [a], Hayato Hikita [a], Naoki Hiramatsu [a], Tatsuya Kanto [a], Norio Hayashi [b], Tetsuo Takehara [a,*]

[a] Department of Gastroenterology and Hepatology, Osaka University Graduate School of Medicine, 2-2, Yamadaoka, Suita 565-0871, Japan
[b] Kansai Rosai Hospital, 3-1-69, Inabaso, Amagasaki 660-8511, Japan

ARTICLE INFO

Article history:
Received 5 July 2011
Available online 23 July 2011

Keywords:
MicroRNA
Hepatitis C virus
PI3 kinase/Akt pathway

ABSTRACT

The aim of this study was to investigate the role of microRNA (miRNA) on hepatitis C virus (HCV) replication in hepatoma cells. Using miRNA array analysis, miR-192/miR-215, miR-194, miR-320, and miR-491 were identified as miRNAs whose expression levels were altered by HCV infection. Among them, miR-192/miR-215 and miR-491 were capable of enhancing replication of the HCV replicon as well as HCV itself. HCV IRES activity or cell proliferation was not increased by forced expression of miR-192/miR-215 or miR-491. Investigation of signaling pathways revealed that miR-491 specifically suppressed the phosphoinositol-3 (PI3) kinase/Akt pathway. Under inhibition of PI3 kinase by LY294002, the suppressive effect of miR-491 on HCV replication was abolished, indicating that suppression of HCV replication by miR-491 was dependent on the PI3 kinase/Akt pathway. miRNAs altered by HCV infection would then affect HCV replication, which implies a complicated mechanism for regulating HCV replication. HCV-induced miRNA may be involved in changes in cellular properties including hepatocarcinogenesis.

1. Introduction

Hepatitis C virus (HCV) is a major causative agent of liver diseases worldwide. Elimination of HCV fails in about 80% of infected patients, which leads to chronic hepatitis, liver cirrhosis, and subsequent development of hepatocellular carcinoma [1]. Combination therapy of pegylated-interferon-α and ribavirin results in sustained clearance of serum HCV-RNA in only ~50% of patients [2,3]. To improve therapeutic efficacy of the virologic response rate, drugs inhibiting the functions of HCV proteins such as NS3, NS5A, and NS5B, are currently under development. Although a number of studies have clarified the mechanisms of the effect of HCV on infected cells or the role of host factors on regulation of HCV replication, there remains much to be investigated.

MicroRNAs (miRNAs) were identified as a population of small RNAs, modulating translation by binding to sites of antisense complementarity in 3′ untranslated regions of target mRNA [4]. With respect to regulation of HCV replication, the relevance of several miRNAs has been recently reported. miR-122, a hepatocyte-specific miRNA, was identified as a positive regulatory factor for HCV replication by binding to two sites in the HCV genome [5]. Each of the interferon-β-induced miRNAs, miR-196, miR-296, miR-351, miR-431, and miR-448, has a partially complementary sequence to HCV, resulting in suppression of HCV replication [6]. Thus, a miRNA with homology to the HCV sequence is likely to have the ability to regulate HCV. Another possible mechanism of miRNA regulation of HCV replication is the targeting of some cellular gene involved in HCV replication. miR-141 was shown to suppress DLC-1 leading to efficient HCV replication [7]. Although some miRNAs were shown to be capable of regulating HCV replication, details of the relationship between miRNAs and HCV replication are still largely unknown.

In the present study, we performed miRNA array analysis to identify miRNA(s) altered by HCV infection in Huh7, a hepatoma cell line. We further investigated whether HCV-regulated miRNA could, in turn, affect HCV replication. As a result, we were able to identify five miRNAs: miR-192 and its homolog miR-215 and miR-194 as upregulated miRNAs and miR-320 and miR-491 as downregulated miRNAs. Among them, miR192/miR-215 and miR-491 enhanced HCV replication in HCV replicon cells as well as in cell culture-infectious HCV (HCVcc)-infected cells. miR-192/miR215 and miR-491 did not increase cell proliferation or HCV internal ribosome entry site (IRES) activity, suggesting that these were not the reasons for increased HCV replication. Further investigation revealed that miR-491 suppressed the PI3 kinase/Akt

* Corresponding author. Fax: +81 6 6879 3629.
E-mail address: takehara@gh.med.osaka-u.ac.jp (T. Takehara).

0006-291X/$ - see front matter © 2011 Elsevier Inc. All rights reserved.
doi:10.1016/j.bbrc.2011.07.049

pathway suggesting that this could be responsible for augmentation of HCV replication by miR-491.

2. Materials and methods

2.1. Cells, antibodies

The hepatoma-derived cell line Huh7 was maintained in DMEM supplemented with 10% FCS. The HCV subgenomic cell line Huh-RepSI, harboring HCV-N (genotype 1b), was previously described [8]. Antibodies to phospho-ERK (Thr202/Tyr204), Akt, phospho-Akt (Ser473) were purchased from Cell Signaling Technology. An antibody to β-actin (A-5441) was from Sigma–Aldrich. A mouse monoclonal antibody to HCV core protein (C7-50) was obtained from Affinity BioReagents. A mouse monoclonal antibody to HCV NS5A (clone 388) was from Meridian Life Science, Inc. LY294002, a PI3 kinase inhibitor, was obtained from Calbiochem.

2.2. Immunoblot analysis

Total cellular protein was extracted with lysis buffer containing 1% Nonidet P-40, 0.5% sodium deoxycholate, 0.1% SDS, 1 mM sodium vanadate, 50 mM NaF, and protease inhibitor cocktail (Nacalai Tesque, Japan) in phosphate-buffered saline. Protein samples were separated by SDS–polyacrylamide gel electrophoresis and transferred to a polyvinylidene difluoride membrane (Bio-Rad). After blocking, the membrane was probed with specific primary antibodies, followed by further incubation with a secondary antibody conjugated with horseradish peroxidase (GE Healthcare). Proteins were visualized using ECL Western blot detection reagents (GE Healthcare) and exposure to film.

2.3. miRNA transfection

Synthesized miRNAs, miR-192, miR-194, miR-215, miR-320, miR-491, and negative control miRNA were purchased from Thermo Fisher Scientific. Cells (2×10^5 per well) were seeded into 6-well plates, transfected with miRNA at a concentration of 10 nM using Lipofectamine RNAiMAX (Invitrogen) according to manufacturer's instruction. After incubation for 2 days, the cells were harvested and assayed by immunoblot or real-time RT-PCR analysis.

2.4. Dual luciferase assay

We used a dicistronic plasmid, pRLHL, to investigate the effects of miRNAs on HCV IRES (Fig. 2A) [9]. Huh7 cells (1×10^6 cells in a 10-cm dish) were transfected with 10 μg of pRLHL using FuGene6 (Roche). After 24 h, the cells were seeded into 24-well plates (5×10^4 cells per well) and transfected with miRNA or negative control at a concentration of 10 nM as described above. After incubation for 2 days, cells were lysed, and assayed for HCV IRES-dependent firefly luciferase activity and cap-dependent renilla luciferase activity using the Dual Luciferase Reporter Assay System (Promega).

2.5. Cell culture-infectious HCV

HJ3-5(YH/QL) is a chimeric cell culture-infectious virus with a genome consisting of the core to NS2 sequence of genotype 1a (H77) virus placed within the background of the genotype 2a JFH1 virus, and containing compensatory mutations in E1 (Y361H) and NS3 (Q1251L) [10]. Virus stock (10^7 focus-forming units (FFU)/ml) was prepared as described previously [11].

For HCV infection, Huh7 cells (2×10^5 per well) were seeded into 6-well plates. After overnight incubation, the medium was replaced with 1 ml medium containing 4×10^5 FFU virus (the infection was carried out at an m.o.i. of ~2). After 12 h incubation, the cells were washed with PBS and re-fed with normal culture medium. At 5 days after inoculation with the virus, total RNA was obtained from the cells using Trizol (Invitrogen).

2.6. Real-time reverse transcription-polymerase chain reaction (RT-PCR)

Total RNA was extracted from the cells with RNAeasy (QIAGEN). The RNA, 1 μg, was reverse transcribed with High Capacity RNA-to-cDNA Master Mix (Applied Biosystems) in a 20 μl reaction, then 1 μl of the reaction was subjected to real-time PCR assay using TaqMan Gene Expression Assays (Applied Biosystems).

2.7. Cell proliferation assay

Cell proliferation was assessed by WST-1 (2-[2-methoxy-4-nitrophenyl]-3-[4-nitrophenyl]-5-[2,4-disulpho-phenyl]-2H-tetrazolium, monosodium salt) assay according to the manufacturer's suggested protocol (Nacalai Tesque). Briefly, Huh7 cells (1×10^4 per well) were seeded into 96-well flat-bottom plates, transfected with synthesized miRNA or negative control as above, and cultured in DMEM containing 10% FBS. WST-1 reagent, 10 μl, was added to each well, the cells were incubated at 37 °C for 1 h, and absorbance at 450 nm was measured using a spectrophotometer.

2.8. miRNA array analysis

To screen for miRNA affected by HCV infection, we performed microarray analysis using *mir*Vana miRNA Bioarray V9.2 (Ambion), which carries genes for a total 633 kinds of miRNAs containing 471 human genes, 380 mouse genes and 238 rat genes. Using the flash PAGE system (Ambion), miRNA was purified from 22 μg total RNA extracted from HCVcc-infected cells or mock-infected cells. The purified miRNA samples from HCVcc-infected cells and mock-infected cells were labeled with Cy3 and Cy5, respectively, using mirVana miRNA Labeling kit (Ambion) and CyeDye Mono-Reactive Dye Pack (GE Healthcare Biosciences). The labeled miRNA was hybridized to the array for ~16 h at 42 °C. After hybridization, the array was washed with Low Stringency Wash (Ambion) once and High Stringency Wash (Ambion) twice. Next, the array was dried with centrifugation at 600*g* for 3 min and scanned with GenePix 4000B scanner (Axon Instruments, CA, USA). The signal data were calculated with an Array-Pro Analyzer ver. 4.5 (Media Cybernetics, Inc.). The array data were normalized by global normalization using the Microarray Data Analysis Tool (Filgen, Inc.).

3. Results

3.1. Identification of miRNAs regulated by HCV infection

Huh7 cells were infected with HCVcc at ~2 m.o.i. After incubation for 5 days, total RNA was extracted from the cells followed by purification with small RNA and miRNA array analysis. A portion of the cells was subjected to immunofluorescence analysis for staining of HCV core protein to verify that more than 90% of the cells were infected with HCV. The ratio of Cy3 intensity to Cy5 intensity was calculated and alteration of the miRNA expression profile was analyzed. A ratio of more than 1.5-fold increase/decrease was considered to be altered. To exclude miRNAs with low expression levels, those with a net intensity of Cy3 and Cy5 of more than 1000 were picked out. As a result, the miRNAs of miR-192, miR-194, miR-320, and miR-491 were identified as altered miRNAs (Table 1). miR-192 and miR-194 were up-regulated by HCV infection,

Table 1
miRNAs altered by HCV infection.

miRNA	Intensity				Sequence
	Cy3 (HCV)	Cy5 (mock)	Net	Cy3/Cy5	
miR-192	987.90	607.05	1594.95	1.63	CUGACCUAUGAAUUGACAGCC
miR-194	793.48	498.00	1291.48	1.59	UGUAACAGCAACUCCAUGUGGA
miR-215	156.21	69.39	225.60	2.25	AUGACCUAUGAAUUGACAGAC
miR-320	897.44	1401.93	2299.37	0.64	AAAAGCUGGGUUGAGAGGGCGAA
miR-491	925.38	2495.47	3420.85	0.37	AGUGGGGAACCCUUCCAUGAGGA

and miR-320 and miR-491 were down-regulated. In addition, miR-215, whose net expression while relatively low, was also studied in the subsequent investigation as an upregulated miRNA because it is considered to be a cousin of miR-192 (see their homologous sequences in Table 1). miR-215 showed a high induction level, and miR-192 and miR-215 were reported to have common induction mechanisms and target genes [12,13].

3.2. Regulation of HCV replication by miRNAs

Next, we checked whether the miRNAs were capable of regulating HCV replication. To assess this, we transfected Huh-RepSI, a HCV subgenomic replicon cell line, with synthesized miRNAs, and then monitored HCV RNA abundance and NS5A protein abundance using real-time RT-PCR and immunoblot analysis, respectively. Among the five miRNAs tested, miR-192/miR-215 and miR-491 significantly increased replicon abundance (Fig. 1A and B), while miR-194 and miR-320 did not show any significant change. HCV subgenomic replicon RNA contains the NS3 through NS5B region, which is required for genome RNA replication, but not for virus particle production. To confirm that the effect of the miRNAs was reproducible in a system equipped with the entire HCV life cycle, we used Huh7 cells infected with HCVcc. As expected, HCV abundance was upregulated by the three miRNAs in the HCVcc-infected cells similarly to HCV replicon cells (Fig. 1C and D). In addition, the HCV strain used in the experiment was a chimera of genotype 1a (H77, core to NS2) and genotype 2 (JFH-1, NS3 to NS5B) [10]. In particular, the genotype of the replication machinery of the virus (namely, NS3 to NS5B) was JFH-1. This differed from that of Huh-RepSI (HCV-N, genotype 1b) [8], which suggests that the enhancing effect of miR-192/miR-215 and miR-491 on HCV genome replication was not genotype-specific.

3.3. Effect of miRNAs on HCV IRES, cell proliferation

Since miR-192/miR-215 and miR-491 were shown to be capable of enhancing HCV replication, we next tried to elucidate how they regulate it. First, we examined whether the miRNAs can regulate HCV IRES activity. In this experiment, we transfected replicon cells with a dicistronic vector, pRLHL [9], which contained the firefly luciferase gene driven by HCV IRES and the renilla luciferase gene translated in a cap-dependent manner which was used as a control of general translational activity (Fig. 2A). After 24 h, the miRNAs were transfected, then luciferase activities induced by HCV IRES and cap translation were measured at 2 days after

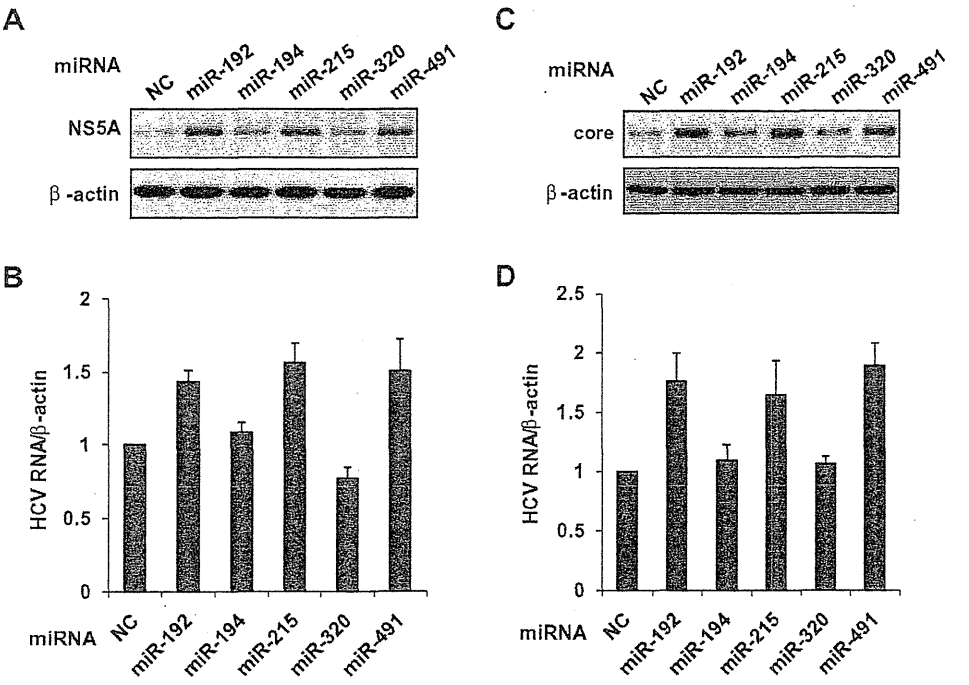

Fig. 1. Regulation of HCV replicon or HCVcc abundance by miRNAs. Cells of Huh-RepSI, a HCV subgenomic replicon, were transfected with synthesized miRNAs and assayed for NS5A protein expression (A) or HCV RNA abundance (B). HCVcc-infected Huh7 cells were transfected with synthesized miRNAs and assayed for core protein expression (C) or HCV RNA abundance (D). NC: negative control miRNA.

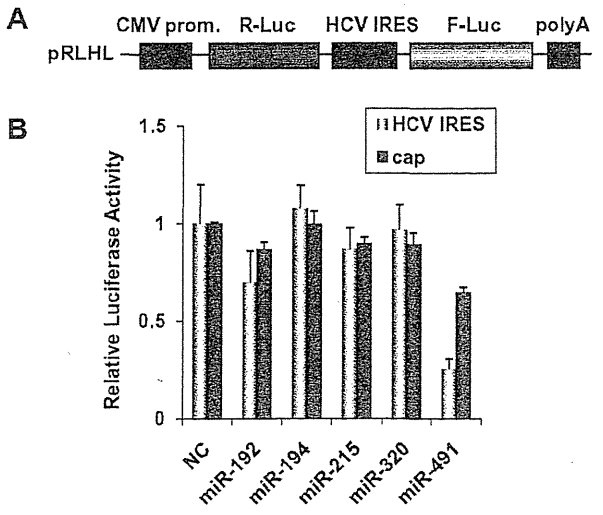

Fig. 2. Regulation of HCV IRES and cap-dependent translation by miRNAs. Huh-RepSI cells were transfected with a dicistronic vector, pRLHL (A), incubated for 24 h. The cells were seeded to 24-well plates and transfected with the miRNAs. After further incubation for 2 days, the cells were harvested and assayed for dual luciferase activity (B).

transfection (Fig. 2B). In this assay, activation of IRES was determined by the ratio of IRES-dependent luciferase activity to cap-dependent luciferase activity. Interestingly, none of the miRNAs could increase the HCV IRES activity. miR-491 suppressed cap-dependent translation and showed more suppression of HCV IRES activity. Thus, these results indicated that there was some mechanism upregulating HCV replication other than regulation of IRES activity.

Previous work demonstrated that HCV replication was affected by cell proliferation [14]. This led us to access the effects of the miRNAs on cell proliferation. Compared to negative control miRNA-transfected cells, however, none of the transfectants of the miRNAs, including those which increased HCV replication, revealed upregulation of cell proliferation, and miR-491 even suppressed it (Fig. 3). Therefore, regulation of cell proliferation was not the reason for the increase of HCV replication. The effect of miR-491 of suppressing cell growth was likely to be caused by inhibition of general translation as shown in Fig. 2B.

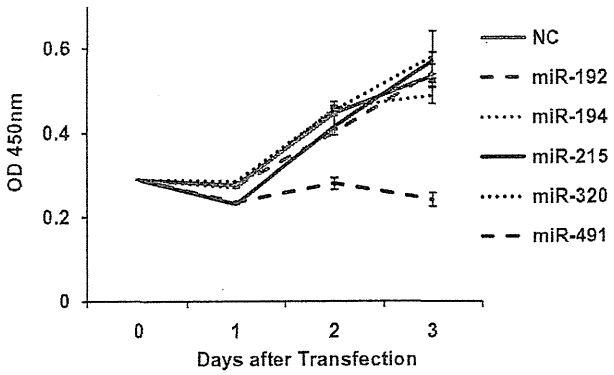

Fig. 3. Regulation of cell proliferation by miRNAs. Huh7 cells were seeded into 96-well plates, transfected with the miRNAs. At day 0, 1, 2, and 3 after transfection, the cells were subjected to WST-1 assay as described in Section 2.

3.4. Effect of miRNAs on intracellular signaling

To clarify the mechanism of the regulation of HCV replication, we next focused our investigation on intracellular signaling pathways. Previous studies have reported that HCV replication is regulated by intracellular signaling pathways, such as ERK [15], p38 [8], PI3 kinase/Akt [11], and smad [16], in addition to JAK/STAT. Since transfection of the miRNAs had no effect on the JAK/STAT signaling pathway (data not shown), we examined the phosphorylation of ERK and Akt. Because both showed a suppressing effect on HCV replication, suppression of the pathway was anticipated in cells in which HCV replication was enhanced. As shown in Fig. 4A, phosphorylation of Akt at Ser-473 was markedly suppressed in the cells transfected with miR-491, while no significant inhibition of ERK activity was observed. To further investigate the relevance of the PI3 kinase/Akt pathway to miR-491-induced upregulation of HCV replication, we used LY294002, a PI3 kinase inhibitor. When the PI3 kinase pathway was blocked by this reagent, the HCV RNA level was enhanced up to 2-fold. miR-491 transfection also resulted in an increase of HCV abundance, though the effect was less

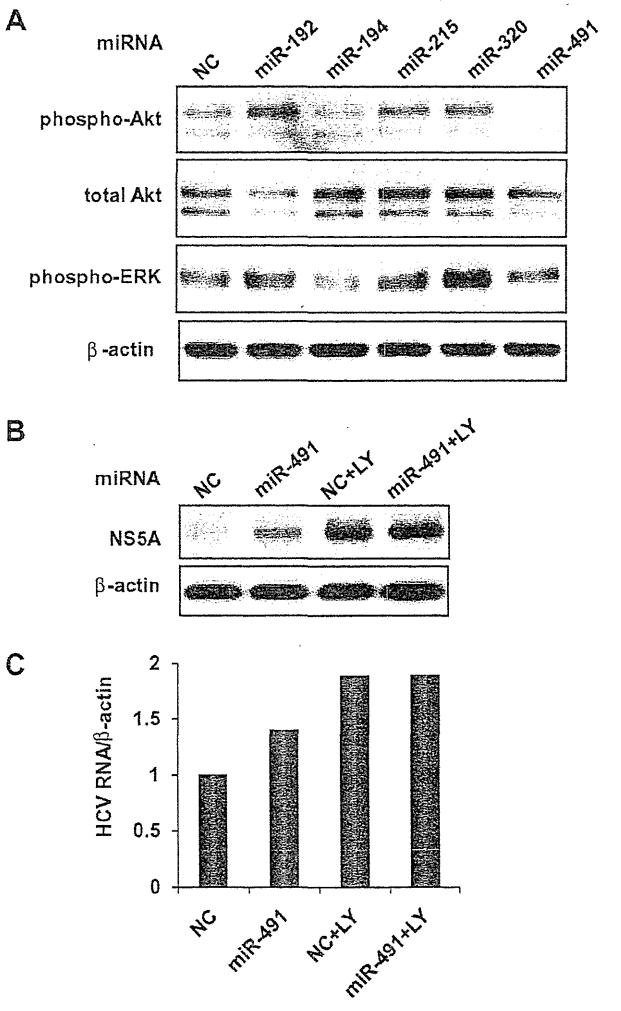

Fig. 4. Involvement of Akt suppression in miR-491-mediated upregulation of HCV replication. (A) Immunoblot analysis of miRNA-transfected HCV replicon cells using antibodies to Akt, phospho-Akt, phospho-ERK and β-actin. (B and C) HCV replicon cells were transfected with miR-491 or treated with Akt inhibitor, and assayed for NS5A protein abundance (B) or HCV RNA abundance (C). LY: LY294002.